SYNTHESIS, CHARACTERISATION, CONFORMATIONAL STUDY AND ANTIBACTERIAL ACTIVITY OF *N*-ACYLHYDRAZONE AND ITS DERIVATIVES

By

TAN YI YING

A project report submitted to the Department of Chemical Sciences,

Faculty of Science,

Universiti Tunku Abdul Rahamn,

In partial fulfilment of requirement for the degree of Bachelor of Science (Honours) Chemistry

May 2023

ABSTRACT

SYNTHESIS, CHARACTERISATION, CONFORMATIONAL STUDY AND ANTIBACTERIAL ACTIVITY OF *N*-ACYLHYDRAZONE AND ITS DERIVATIVES

TAN YI YING

Researchers had examined *N*-acylhydrazone in great detail because of their pharmacological activities. For instance, *N*-acylhydrazone is found to be able to act as an antibacterial, anti-inflammatory, anticancer, anticonvulsant, antimalarial as well as antiplatelet aggregation agent. This project has successfully synthesised a carboxylic acid hydrazide and a total of ten new *N*-acylhydrazone derivatives. The carboxylic acid hydrazide was prepared from the condensation of a carbonyl ester group and hydrazine hydrate. The carboxylic acid hydrazide produced was then reacted with various types of benzaldehyde to generate a wide variety of *N*-acylhydrazone derivatives. The ten compounds were synthesised with yields ranging from 35 to 74 %. The chemical structure of the generated carboxylic acid hydrazide and ten new *N*-acylhydrazone derivatives were elucidated with the help of FT-IR, ^{1}H NMR, ^{13}C NMR, NOE, DEPT, HMQC and HMBC. From the spectral data obtained, it was concluded that the predominant stereoisomer of the products is with (*E*) configuration and *cis* conformer. In addition, the energy for the rotational barrier for the compounds investigated were ranged 75.26 kJ mol^{-1}. Besides, it

was found that *N*-acylhydrazone SB (substituted) exhibited excellent antibacterial activity against *Bacillus subtilis* and *Staphylococcus aureus* with the MIC value of 31.25 μg/mL and 15.63 μg/mL, respectively by using the broth dilution method.

ABSTRAK

SINTESIS, KARAKTERISASI, ANALISIS KONFORMASI, AKTIVITI ANTIBAKTERIA BAGI N-ACYLHYDRAZONE DAN DERIVATIFNYA

TAN YI YING

N-acylhydrazone telah dikaji secara meluas oleh penyelidik kerana dia mempunyai banyak aktivit terapeutik. Sebagai contoh, *N*-acylhydrazone boleh menjadi ejen antibakteria, anti-inflamasi, anti-kanser, antikonvulsan, anti-malaria dan antiplatelet agregasi. Dalam projek ini, satu hidrazida asid karboksilik dan sepuluh derivatif *N*-acylhydrazones telah disintesis. Hidrazida asid karboksilik boleh dihasilkan melalui hidrazin hidrat dengan kumpulan karbonil. Selain itu, hidrazida asid karboksilik yang disediakan boleh bertindakbalas dengan benzaldehida yang berlainan untuk menghasilkan derivatif *N*-acylhydrazones. Peratusan hasil derivatif *N*-acylhydrazones yang disediakan adalah antara 35 hingga 74 %. Hidrazida asid karboksilik dan derivatif *N*-acylhydrazones telah dicirikan dengan menggunakan pelbagai instrument seperti FT-IR, ^{1}H NMR, ^{13}C NMR, NOE, DEPT, HMQC dan HMBC. Di samping itu, kebanyakan produk yang dihaliskan memiliki (*E*) konfigurasi dan *cis* konformer. Tambahan pula, produk yang disintesis mempunyai halangan putaran antara 75.26 kJ mol^{-1}. Seterusnya, *N*-acylhydrazone SB mempunyai aktiviti antibakteria yang baik ke atas dua

strain bakteria seperti *Bacillus subtilis* (MIC value: 31.25 μg/mL) dan *Staphylococcus aureus* (MIC value: 15.63 μg/mL).

ACKNOWLEDGEMENT

I received a lot of support and help through this final year project. First and foremost, I would like to express my special thanks of gratitude to my supervisor, Dr. Sim Kooi Mow, whose knowledge was essential in generating this research title and methodology. The project could be carried out successfully and smoothly because of his leadership and perseverance at each stage of the procedure. His kindness and willingness to impart his knowledge had allowed me to learn new things and knowledge that went beyond our syllabus and course materials. Moreover, I wish to express my gratitude towards my co-supervisor, Dr. Teo Kah Cheng, who assists me a lot in the antibacterial assay.

Furthermore, I would like to thank all the laboratory officials for their useful advice and courteous assistance throughout this final year project.

Additionally, my thanks and appreciation also go to my parents and friends, especially my lab mate (Khong Pek Yao) as they always support and encourage me during the study for this project.

Last but not least, I sincerely thank UTAR for providing a such comfortable environment for me to conduct my final year project successfully.

DECLARATION

I hereby declare that the project report is based on my original work except for quotations and citations which have been duly acknowledged. I also declare that it has not been previously or concurrently submitted for any other degree at UTAR or other institutions.

Name: TAN YI YING

Date : 26/5/2023

APPROVAL SHEET

This project report entitled "**SYNTHESIS, CHARACTERISATION, CONFORMATIONAL STUDY AND ANTIBACTERIAL ACTIVITY OF *N*-ACYLHYDRAZONE AND ITS DERIVATIVES**" was prepared by TAN YI YING and submitted as partial fulfilment of the requirements for the degree of Bachelor of Science (Honours) Chemistry at Universiti Tunku Abdul Rahman.

Approved by,

Supervisor

KM SIM

---------- Date: 26/5/2023

(DR. SIM KOOI MOW)

Associate Professor

Department of Chemical Science

Faculty of Science

University Tunku Abdul Rahman

FACULTY OF SCIENCE

UNIVERSITI TUNU ABDUL RAHMAN

Date: 26/5/2023

PERMISSION SHEET

It is hereby certified that **TAN YI YING** (ID No: 19ADB01241) has completed this final year project entitled "**SYNTHESIS, CHARACTERISATION, CONFORMATIONAL STUDY AND ANTIBACTERIAL ACTIVITY OF *N*-ACYLHYDRAZONE AND ITS DERIVATIVES**" under the supervision of DR. SIM KOOI MOW from Department of Chemical Science, Faculty of Science and DR. TEO KAH CHENG from Department of Agricultural and Food Science, Faculty of Science.

I hereby give permission to the University to upload the softcopy of my final year project in pdf format into UTAR Institutional Repository, which may be made accessible to the UTAR community and public.

Yours truly,

_____

(TAN YI YING)

TABLE OF CONTENTS

LIST OF TABLES

LIST OF FIGURES

LIST OF SCHEMES

LIST OF SYMBOLS/ABBREVIATIONS

mmol	Millimole
g mol^{-1}	Molecular weight
µg mL^{-1}	Microgram per millimetre
mM	Millimolar
SB	Schiff base
NAH	*N*-acylhydrazone
TLC	Thin Layer Chromatography
R_f	Retention factor
kJ mol^{-1}	Kilojoule per mole
FT-IR	Fourier Transform Infrared Spectroscopy
nm	Wavelength
1D-NMR	One dimensional Nuclear Magnetic Resonance
2D-NMR	Two dimensional Nuclear Magnetic Resonance
DEPT	Distortionless Enhancement by Polarization Transfer
HMQC	Heteronuclear Multiple Quantum Correlation
HMBC	Heteronuclear Multiple Bond Correlation
NOE	Nuclear Overhauser Effect
Hz	Herts
J	Coupling constant
s	Singlet
br s	Broad singlet
d	doublet

dd	Doublet of doublets
m	Multiplet
δ	Chemical shift
δ_C	Chemical shift of carbon
δ_H	Chemical shift of hydrogen
T_C	Coalescence temperature
Δv	Peak separation
k_C	Rate constant of *cis/trans* equilibrium
$\Delta G^{\neq}$	Energy of rotational barrier
MIC	Minimum Inhibitory Concentration
ATCC	American Type Culture Collection
MH	Mueller-Hinton
cfu	Colony forming unit

CHAPTER 1

INTRODUCTION

1.1 Indole

Indole is a naturally occurring chemical compound where one five-membered pyrrole ring is fused with one six-membered benzene ring. Thus, it is also known as benzopyrrole which is under the category of alkaloid. **Figure 1.1** illustrates the basic structure of an indole. This bicyclic organic molecule is considered as aromatic because there is continuous conjugation of double bonds. Besides that, indole also fulfils the Hückel rule (4N+2) and thus has a total of 10 π electrons. It has the general formula of C_8H_7N and a molecular weight of 117.15 g mol^{-1}. Indole is a naturally occurring secondary metabolite and can be found in the human intestine as well as flower essential oils such as orange blossom and jasmine (Jagadeesan and Karpagam, 2022).

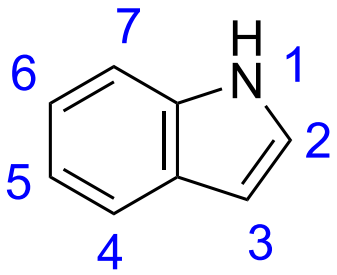

Figure 1.1: Basic structure of an indole

1.1.1 Application of indole

Indole is widely used due to its prominent characteristics, for instance, anti-inflammatory, anti-allergic, anti-tubercular, antitumour, anticonvulsant and anti-microorganism properties (Jagadeesan and Karpagam, 2022). Indole has the ability to fit and bind to many receptors. Apart from that, compounds that consist of an indole group such as etodolac and osimertinib can function as non-steroidal anti-inflammatory drugs (NSAID) and antineoplastic drugs respectively. Besides, serotonin acts as a neurotransmitter to maintain the body's health (Govaerts, et al., 2022). **Figure 1.2** lists examples of chemical compounds consisting of indole group and their usage.

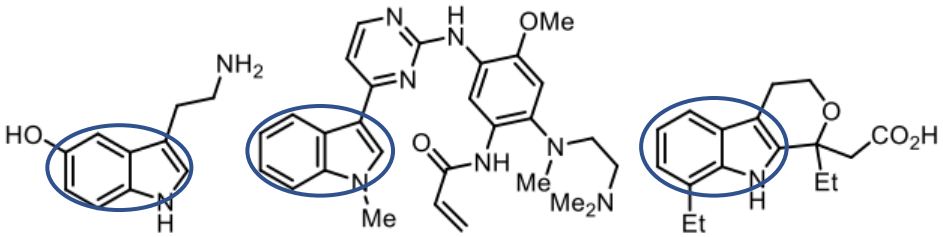

Figure 1.2: Examples of chemical compounds consist of indole group and their usage

1.1.1.1 Antibacterial Activity of Indole

Indole-containing compounds were found to have antibacterial activity on Gram-positive bacteria strain such as *Staphylococcus aureus*, *Mycobacterium tuberculosis* as well as *Bacillus subtilis*. For instance, according to the research done by Yuan and his group, a newly synthesised compound that contains

indole is able to suppress the bacterial strains from growing by affecting the Filamenting temperature-sensitive mutant Z (FtsZ) polymerisation reaction. FtsZ is the protein that is important in the cell division process in bacteria. In short, indole-containing compounds will lead to bacteria cell death (Yuan, et al., 2019).

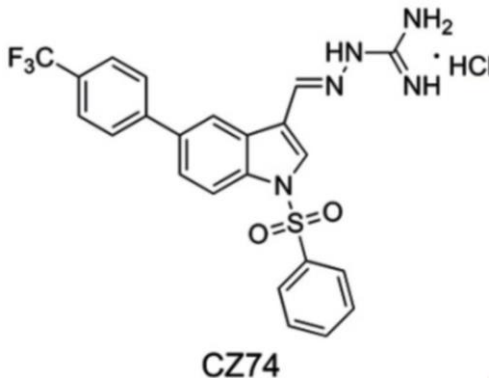

CZ74

Figure 1.3: CZ74, the newly synthesised compound that has antibacterial activity (Yuan, et al., 2019)

1.1.1.2 Anti-inflammatory Activity of Indole

Inflammation is a process whereby the human immune system detects and gets rid of foreign molecules from the body and at the same time starts the healing progress. Indole is often incorporated into non-steroidal anti-inflammatory drugs (NSAIDs). Besides etodolac and osimertinib, indomethacin, a methylated indole is also functioned as a painkiller to treat swelling, fever and also pain. Furthermore, diseases such as osteoarthritis as well as rheumatoid arthritis can be cured by using drugs likewise etodolac and acemetacin. The chemical structures of the biologically active compounds that have anti-inflammatory activity are shown in **Figure 1.4** (Song, et al., 2019).

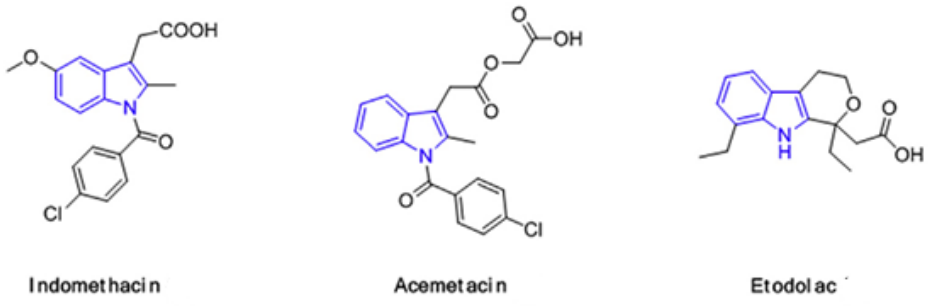

Figure 1.4: Chemical structure of compounds that have anti-inflammatory activity (Song, et al., 2019)

1.1.1.3 Antitumour Activity of Indole

Apart from that, indole also exhibits anticancer properties. Indole-containing compounds managed to inhibit various types of enzymes that involve in gene regulation. For example, indole plays an important role in the histone deacetylases (HDACs) suppressor. According to the research done by Dadashpour's group, it was found that the presence of a 5-fluoro substituent in the indole heterocyclic ring will greatly enhance the cytotoxicity of the compound. Besides, eudistomin K with the indole ring had become the lead compound in generating the antitumor agents (Dadashpour and Emami, 2018).

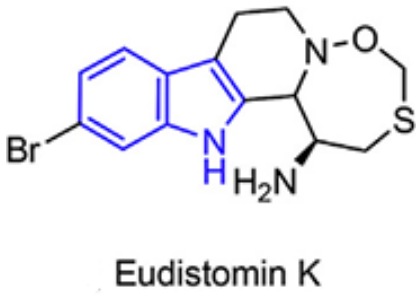

Figure 1.5: Chemical structure of the lead compound, eudistomin K that contains an indole ring (Dadashpour and Emami, 2018)

1.2 Hydrazide

Hydrazide is a functional group that consists of acyl or alkyl groups bounded to $NHNH_2$ groups. **Figure 1.6** below showed the general structure of hydrazide. The R group can be replaced by ester groups, acyl halides as well as cyclic anhydrides. Hydrazide is an essential functional group in medicinal chemistry.

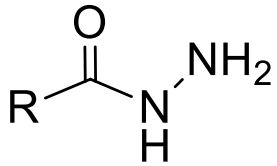

Figure 1.6: General structure of hydrazide

1.2.1 Application of hydrazide

The presence of free available proton in the NH_2 group contributes to the biological activity of hydrazide. For instance, hydrazide and its derivatives are used as anti-inflammatory, antimicrobial, antineoplastic and antidiabetic drugs. Isonicotinic acid hydrazide (INH) is one example of acid hydrazide that has remarkable therapeutic properties. Besides that, hydrazide will undergo a condensation reaction with carbonyl groups to produce hydrazone. Hydrazone is said to be safer than hydrazide. This is because, in hydrazone, the amino group is unable to move freely (Khan, Siddiqui and Tarannum, 2017).

1.2.1.1 Antimicrobial Activity of Hydrazide

In fact, hydrazides with different substituents will have different clinical properties. For example, the group of Kaplancikli revealed that pyrazine-based hydrazides have effective antimicrobial activity on the plant pathogens, *Plasmopara viticola* as well as *Phomopsis obscurans* (fungi) in plants (Kaplancikli, et al., 2010; as cited in Khan, Siddiqui and Tarannum, 2017). It was found that the changes in the substituents on the phenyl ring will affect the biological properties of the compound.

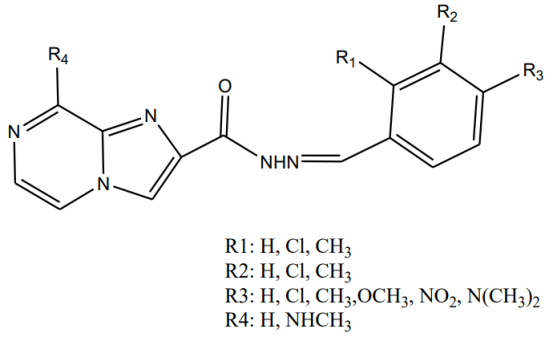

Figure 1.7: Structure of pyrazine-based hydrazine (Khan, Siddiqui and Tarannum, 2017)

1.2.1.2 Anti-inflammatory Activity of Hydrazide

Furthermore, pyrazine-based hydrazide has been found to have anti-inflammatory characteristics too. It is able to prevent the enzymatic activity of inducible nitric oxide synthase (iNOS) as well as the nuclear factor kappa B (NF-κB). For instance, β-*N*-(4-methylphenylsulphonyl) hydrazide that formed after ring opening exhibited anti-inflammatory properties (Khan, Siddiqui and Tarannum, 2017). The reaction scheme is shown below.

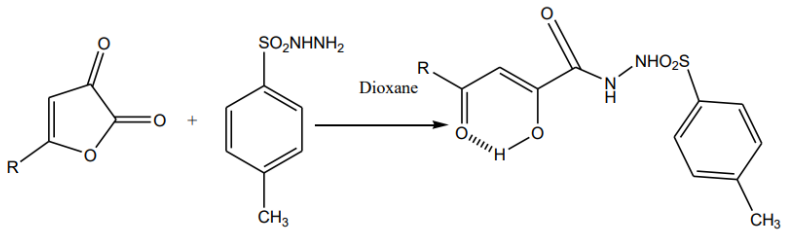

Scheme 1.1: Formation of β-*N*-(4-methylphenylsulphonyl) hydrazide with anti-inflammatory properties (Khan, Siddiqui and Tarannum, 2017)

1.3 Schiff Base

Schiff base (SB) is an organic compound that consists of the azomethine or imine, C=N functional group in the structure. Generally, SB is produced when a carbonyl group react with primary amine through the condensation reaction. This reaction will eliminate one water molecule as the by-product. It has a general formula of $R_2C=NR'$ where R and R' can be either aryl or alkyl groups. The presence of the aryl group enhances the stability of the SB compound generated as compared to the alkyl group. Aliphatic SB compound will undergo polymerisation easily as it is unstable. On the other hand, aromatic SB compound experience conjugation over the ring and hence will be more stable (Hussain, et al., 2016).

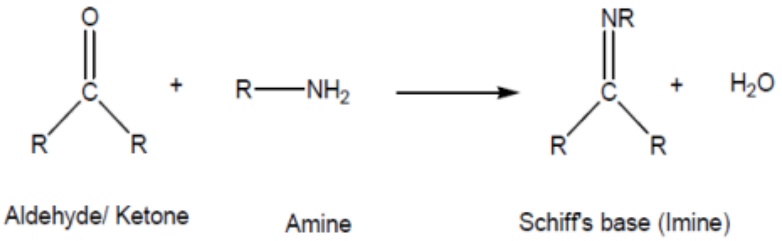

Scheme 1.2: Condensation reaction to produce Schiff base (Hussain, et al., 2016)

Additionally, Schiff base can be synthesised through the reaction between heterocyclic aromatic ring and chitosan. The desired product formed is relatively stable and exhibits various types of biological properties (Haj, Mohammed and Mohammood, 2020). Furthermore, SB can also be produced through the green synthesis pathway by utilising microwave irradiation. For instance, naphthalene-2,3-diamine reacted with the excess reagent of 1*H*-pyrrole-2-cabaldehyde under microwave irradiation to produce (*N*,*N*'-bis(1*H*-pyrrole-2yl) methylene naphthalene-2,3-diimine (BPND). This reaction takes less than 15 minutes to complete. Alternatively, the formation of the metal-SB ligand complex can be also done by using microwave irradiation. Microwave irradiation acts as a greener source of energy and it is able to reduce the time of reaction required (Moeketse, et al., 2022).

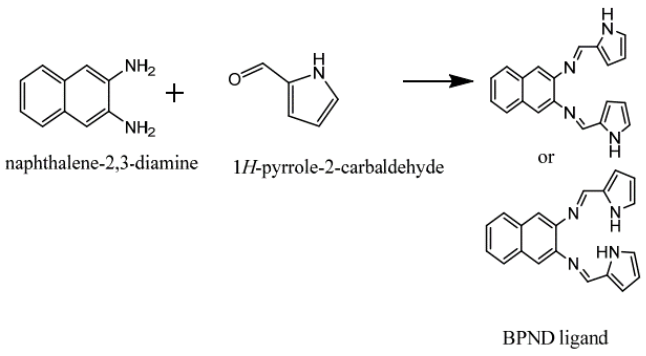

Scheme 1.3: Synthesis of BPND, Schiff base ligand (Moeketse, et al., 2022)

1.3.1 Application of Schiff Base

The Schiff base often appears as a catalyst in the chemical reaction. For example, the fixation process of carbon dioxide is catalysed by Schiff base in order to reduce the accumulation of this gas in the surrounding. Moreover, Schiff base (SB) frequently functions as ligands to coordinate with different types of metal to form metal-ligand complexes. A strong interaction is found between SB and the metal ions. The π-acceptor characteristic of SB allows it to accept electrons from the metal ions (Ceramella, et al., 2022). For example, Sb can coordinate with metals such as copper, nickel as well as lanthanide metals (Moeketse, et al., 2022). This chelation ability enables the SB-metal complex to show biological activities.

1.3.1.1 Antibacterial Activity of Schiff Base

According to the research done, the Schiff base compounds generated have greater antibacterial activity against *Staphylococcus epidermidis* than that of ciprofloxacin, an antibiotic drug (Ceramella, et al., 2022). The MIC value for the SB compound is recorded as 7.81 μg/mL while that of the ciprofloxacin is 15.62 μg/mL. Besides, it was found that the antibacterial activity of the Schiff-base-copper complex had been elevated by 472 % for *Escherichia coli* and 823 % for *Staphylococcus aureus* bacteria strain when compared to the Schiff base ligand alone. The biologically active properties of Schiff base are believed to be contributed by the keto-enol tautomerisation that occurs in the SB compounds. Additionally, SB compounds in nanoparticle size will lead to

stronger antibacterial properties against *Staphylococcus aureus* (Ceramella, et al., 2022).

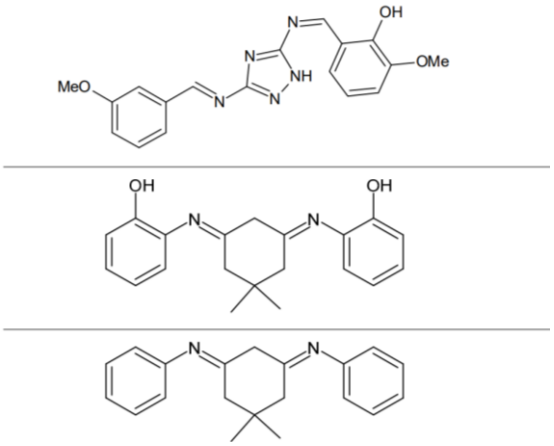

Figure 1.8: Compounds that have stronger antibacterial activity than the ciprofloxacin, antibiotic (Ceramella, et al., 2022)

1.3.1.2 Antioxidant Activity of Schiff Base

Schiff base exhibits antioxidant activity and this property is normally evaluated by using a DPPH assay. Antioxidant activity refers to the inhibition of the oxidation reaction of the compound. By referring to the research done, it can be concluded that the Schiff base-copper chelate exhibited stronger antioxidant activity than the Schiff base compound alone (Shah, et al., 2020).

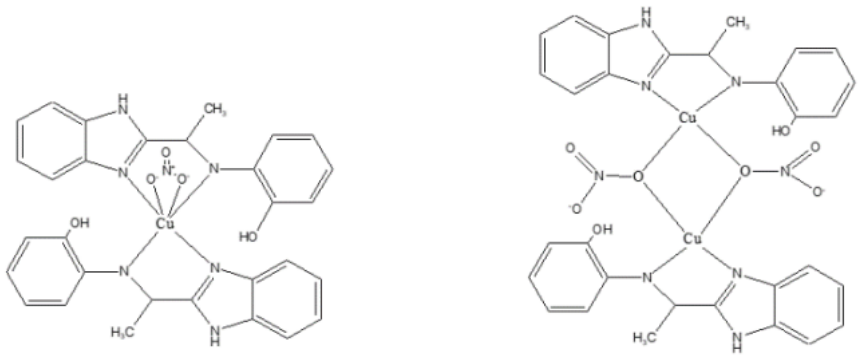

Figure 1.9: Chelation of Schiff base-Copper complex that have stronger antioxidant activity (Shah, et al., 2020)

1.3.1.3 Antitumour Activity of Schiff Base

The Schiff base-metal chelate managed to prevent the cell proliferation process and thus exhibits anticancer characteristics. For example, a Schiff base-Cadmium complex successfully suppressed the cell division process in the breast tumour cell. One nitrogen atom from pyridine rings, another nitrogen atom from the imine bond and also one carboxylate oxygen from each of the two SB ligands will coordinate to the central cadmium ion, forming stable chelation. The six-coordinate chelate synthesised is determined to have greater inhibitory action than the usual chemotherapy drug, cisplatin on the breast tumour (Malik, et al., 2018).

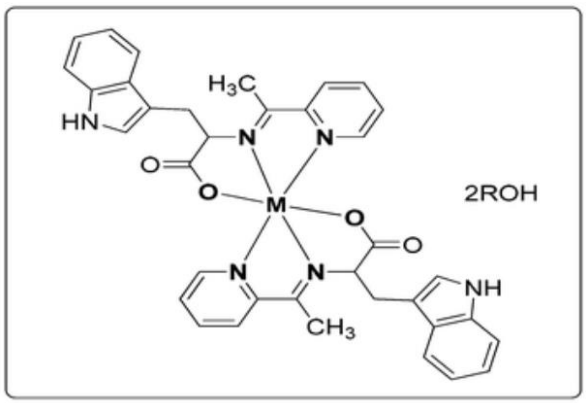

M = Cu **(2.68)**, Zn **(2.69)** and Cd **(2.70)**

Figure 1.10: Chemical Structure of Schiff Base-Cadmium chelate (Malik, et al., 2018)

1.4 Hydrazone

Hydrazone is an organic molecule that consists of a carbon atom that forms a double bond with the N-NH_2 group. **Figure 5** below shows the chemical structure of hydrazone. *N*-acylhydrazone, which is the desired product of this research, is produced through a series of reactions. The chemical reactions usually involves the condensation reaction between hydrazide and compound with carbonyl functional groups (ketone and aldehyde). One molecule of water will be eliminated as a by-product during this condensation reaction. There are two types of nitrogen atoms present in hydrazone. Both nitrogen atoms are nucleophilic and have the capability to donate their electrons. However, the nitrogen in the amino group (NH_2) has a higher reactivity. Furthermore, the carbon atom is able to act as a nucleophile as well as an electrophile. Moreover, the C=N can conjugate with the electron lone pair on the terminal nitrogen

atom. This contributes to the distinct chemical and physical characteristics of hydrazone (Tok, et al., 2021). Hydrazone become the interest of study as it managed to undergo many ring closure reactions (Rasheed, et al., 2014).

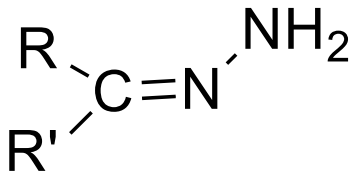

Figure 1.11: Basic structure of hydrazone

1.4.1 Application of *N*-acylhydrazone

According to the research done, *N*-acylhydrazone is bioactive and has become part of the structure of many lead compounds in the medicinal field. For instance, the derivatives of 2-nitrofuran semicarbazones, are functioned as antibacterial drugs. Nitrofurantoin is an antibiotic medication where this orally taken drug can effectively cure urinary tract infections (Thota, et al., 2018).

1.4.1.1 Antibacterial activity of *N*-acylhydrazone

Besides that, nitrofurazone, produced through the condensation reaction of 5-nitrofuraldehyde and semicarbazide, is a pale-yellow powder that can be used to suppress the growth of Gram-positive as well as Gram-negative bacteria (National Center for Biotechnology Information, 2022).

1.4.1.2 Anti-inflammatory activity of *N*-acylhydrazone

Furthermore, the condensation product of carboxylic acid hydrazide and 4-[2-(4-methyl-2-phenyl-thiazole-5-yl)-2-oxo-ethoxy]-benzaldehyde showed positive results in the anti-inflammatory activity that take place inside the body. The *N*-acylhydrazone compounds managed to retard the production of nitric oxide synthase (iNOS). It was found that the anti-inflammatory effect of acylhydrazone compound is more powerful than meloxicam, a typical anti-inflammatory drug used in the medicinal field (Khan, Siddiqui and Tarannum, 2017).

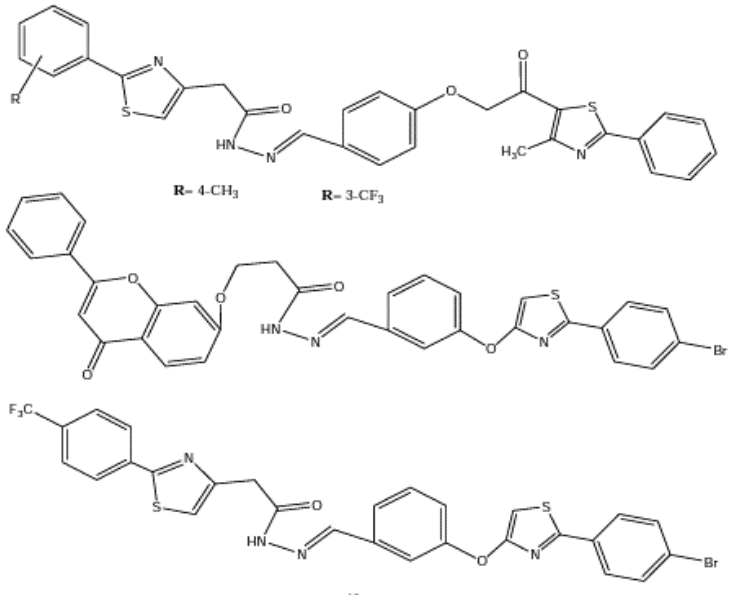

Figure 1.12: Compounds that have stronger anti-inflammatory effects than meloxicam (Khan, Siddiqui and Tarannum, 2017)

1.4.1.3 Antitumour Activity of *N*-acylhydrazone

Furthermore, under the investigation of Kotali and his group, 7-Hydroxy-8-acetylcoumarin benzoylhydrazone is trusted to have anticancer characteristics (Kotal, et al., 2008; as cited in Khan, Siddiqui and Tarannum, 2017).

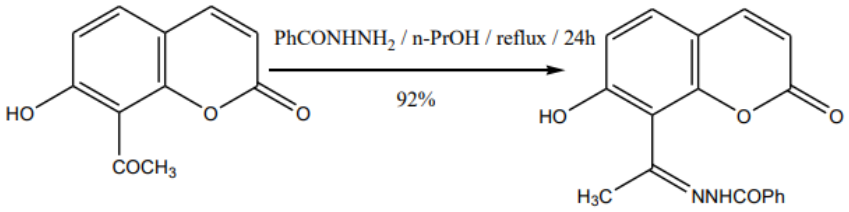

Scheme 1.4: Formation of 7-Hydroxy-8-acetylcoumarin benzoylhydrazone (Kotal, et al., 2008; as cited in Khan, Siddiqui and Tarannum, 2017)

1.4.1.4 Inhibition of enzymatic reaction

Apart from that, amide-based hydrazone derivatives with 2,6-dichlorophenyl substituents were discovered to have a prominent inhibitory effect on monoamine oxidase A (MAO-A), which is an enzyme that breakdown neurotransmitters through the oxidative deamination process (Tok, et al., 2021).

1.5 Antibacterial Activity

Antibacterial activity refers to the ability of the compound to inhibit the growth of bacteria and suppress bacterial activity. More new compounds were synthesised and examined for their antibacterial activity as more bacteria began to develop resistance to the existing drugs. There are various types of techniques that can be used to evaluate the compounds' antibacterial activity. For instance, the dilution method, diffusion as well as Thin Layer Chromatography (TLC)-bioautography method. The dilution method allows the qualitative and quantitative determination of the *in vitro* antibacterial activity. There are two types of dilution methods available which are agar dilution and broth dilution methods. Besides, in the diffusion method, the antibacterial compound will diffuse into the agar medium and thus suppress the growth of the bacteria strain. Furthermore, the TLC-bioautography method involves both chemical and also biological detection techniques. Direct bioautography is more often used to evaluate the antibacterial activity against Gram-positive bacteria such as *Bacillus subtilis* and *Staphylococcus aureus* as well as Gram-negative bacteria which is *Escherichia coli* (Balouiri, Sadiki and Ignsouda, 2016).

1.5.1 Determination of Minimum Inhibitory Concentration (MIC)

The lowest concentration of the antibacterial agent tested that managed to suppress the visible growth of the bacterial strain is named as MIC value. The MIC value can be determined through various types of methods. The dilution method is considered the most accurate technique to determine MIC value. On the other hand, the diffusion method is not considered the best method as it is unable to determine the quantity of the antibacterial agent that diffuses into the agar plate. Among the dilution method, the broth dilution method of either microdilution or macrodilution is frequently used to evaluate the antibacterial activity. The difference between the macrodilution method and microdilution method is in terms of the volume of the mixture used. Macrodilution requires at least 2 mL of growth medium to be present in the tube. Since microdilution requires a very small amount of growth medium, a 96-well plate will be used (Balouiri, Sadiki and Ignsouda, 2016).

1.6 Objectives of the Research

1. To synthesise a carboxylic acid hydrazide, *N*-acylhydrazone and its derivatives.

2. To characterise the structure of carboxylic acid hydrazide, *N*-acylhydrazone and its derivatives by using various spectroscopic techniques, such as FT-IR, 1D-NMR (^{1}H NMR, ^{13}C NMR, DEPT) and 2D-NMR (HMQC, HMBC).

3. To determine the relative configuration of the imine double bond and amide group of *N*-acylhydrazone by using NOE experiments.

4. To determine the rotational barriers around the N-C(O) bond for *N*-acylhydrazone by using Dynamic NMR experiments.

5. To evaluate the antibacterial activity of the *N*-acylhydrazone and its derivatives by using the broth dilution method.

CHAPTER 2

LITERATURE REVIEW

2.1 Synthesis of Indole

Indole can be produced through various types of methods. The most well-established method will be the Fischer indole synthesis. The first step of this total synthesis involved the condensation reactions of phenyl hydrazine and carbonyl groups (ketone and aldehyde) under acidic conditions. Then, the phenylhydrazone produced will undergo rearrangement to form enamine. Enamine will then experience [3,3]-sigmatropic rearrangement as well as protonation of phenyl nitrogen. Then, the cyclic aminal will form and after the removal of one molecule of NH_3, aromatic indole is successfully produced (Humphrey and Kuethe, 2006). The indole synthesised was normally substituted at number 2 or 3-positions (Rahaman, et al., 2021). **Scheme 2.1** describes the reaction mechanism of Fischer indole synthesis (Humphrey and Kuethe, 2006).

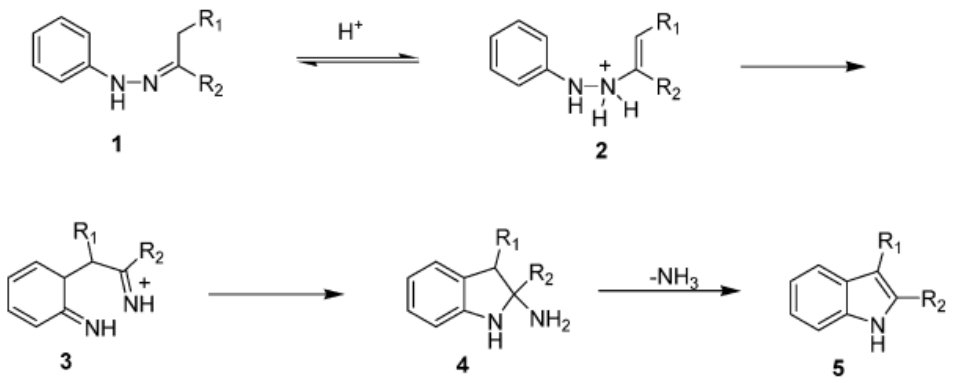

Scheme 2.1: Reaction Mechanism of Fischer indole synthesis (Humphrey and Kuethe, 2006)

2.1.1. Conventional Method

Fischer indole synthesis was investigated by Emil Fischer in 1883. It is one of the most famous and widely used methods to synthesise indole in the pharmaceutical industry. In this method, aryl hydrazine would react with carbonyl groups (aldehyde or ketone) through the condensation process to produce a hydrazone group. The hydrazone then experienced cyclization in the acidic medium at a high temperature to form an indole compound. The homogenous catalysts utilised in this reaction will be Lewis's acid or Bronsted acid (Govaerts, et al., 2022). For instance, Lewis's acids such as $AlCl_3$, BF_3, $FeCl_3$ and $ZnCl_2$ and also Bronsted acid likewise H_2SO_4, HCl and *p*-toluene sulfonic acid are effective in increasing the rate of reaction (Heravi, et al., 2017). **Scheme 2.2** illustrates the classical Fisher Indole Synthesis pathway.

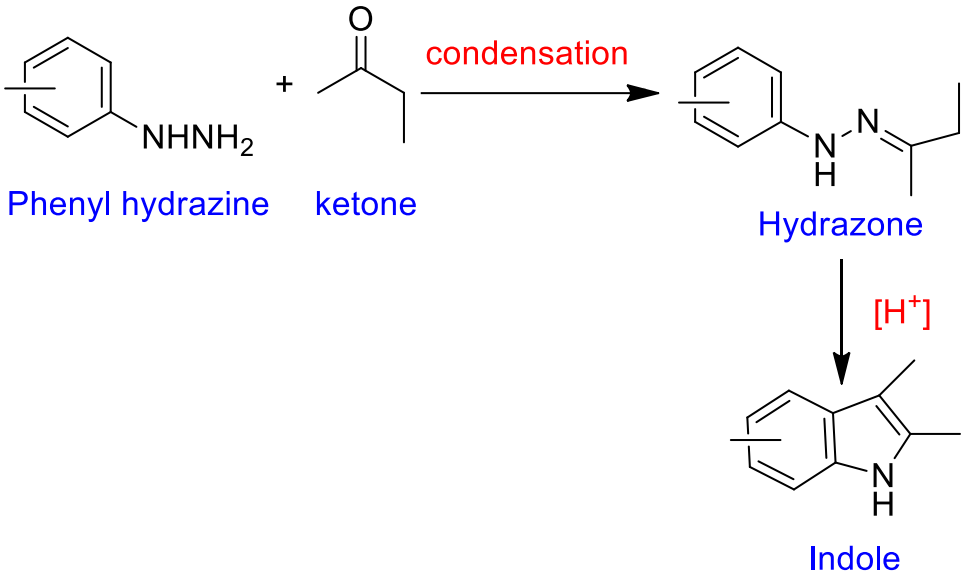

Sche**me 2.2**: Classical pathway of Fisher Indole Synthesis

2.1.2 Green Method

Apart from that, a greener Fischer indole synthesis had been developed by using a conductively heated sealed-vessel reactor (Cirillo, Caccavale and DeLuna, 2020). This reactor had a similar function as the microwave reactor, but it is much cheaper. Besides that, another advantage of using the conductively heated sealed-vessel reactor includes the relatively shorter reaction time when compared to the traditional Fischer indole synthesis. The traditional way requires the reactants to be refluxed for 7 to 8 hours but this greener way only took less than half an hour. The researchers also adopted a more economical and easily available compounds such as dehydroepiandrosterone (DHEA) acetate and phenyl hydrazine as the reactants. The reaction took place at 160 ^{o}C for 20 minutes. The percentage yield of the

products formed ranged from 40% to 60%. Scheme 2.3 showed the reaction pathway of the clean Fischer indole synthesis (Cirillo, Caccavale and DeLuna, 2020).

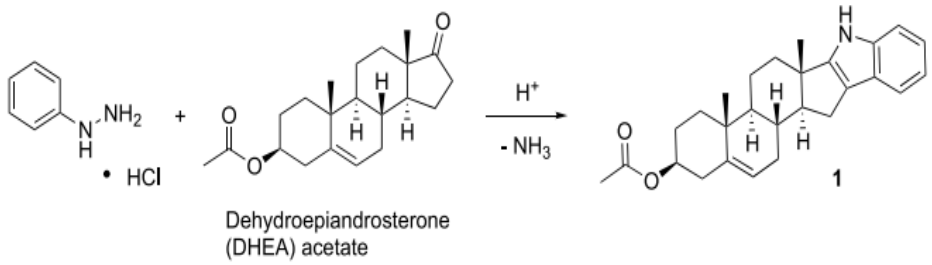

Scheme 2.3: Reaction Pathway of Greener Fischer indole synthesis (Cirillo, Caccavale and DeLuna, 2020)

2.2 Synthesis of carboxylic acid hydrazide

Carboxylic acid hydrazide can be synthesised through the reaction between the ethyl ester of carboxylic acid and hydrazide monohydrate. Hydrazine monohydrate functioned as the nucleophile in this case to attack the carbonyl group of the carboxylate ester. This reaction happened because hydrazine contains lone pair electrons that are able to donate to the electron-deficient species such as the carbon of the carbonyl group which bears a partial positive charge. After that, a tetrahedral intermediate with an alkoxide ion is generated. This intermediate will undergo deprotonation to donate one proton to the alkoxide leaving group and itself becomes carboxylic acid hydrazide.

According to the reaction scheme shown below, different types of R groups in the carboxylic acid could be used to produce a wide variety of carboxylic acid hydrazide. For instance, the R group could be methyl, 1,2-dichloroethyl, 1,2-dibromoethyl as well as benzyl. Besides, ethanol was first used to dissolve the ester of carboxylic acid. The mixture of an ester of carboxylic acid and hydrazide monohydrate was refluxed for two hours. After reflux, the mixture was cooled to ambient temperature and allowed to precipitate. The precipitate produced was obtained through filtration and the crude product was recrystallized from ethanol. The structure of the compound synthesised was elucidated by using ^{1}H NMR as well as ^{13}C NMR (Popiolek and Biernasiuk, 2017).

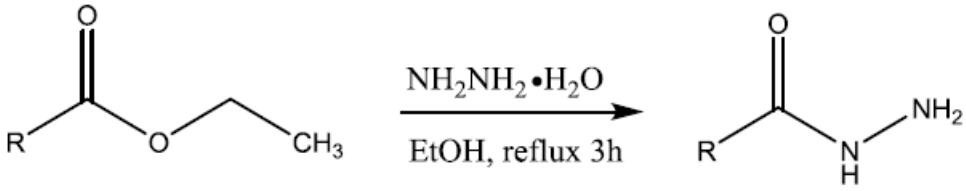

Scheme 2.4: Reaction pathway to synthesis of carboxylic acid hydrazide (Popiolek and Biernasiuk, 2017)

2.2.1 Conventional Method

2.86 mmol of indole-based carboxylate ester was reacted with excess hydrazine monohydrate (43.6 mmol) in 0.5 mL of ethanol. By changing the types of indole carboxylate ester (Compounds 1 and 4) used, different carboxylic acid hydrazide compounds were synthesised. This hydrazinolysis

reaction was carried out at 80 ºC for two hours with continuous stirring. The progress of the reaction was monitored by using Thin Layer Chromatography (TLC) method. After the reaction was completed, the mixture was cooled with the help of ice water. The precipitate formed was then obtained through filtration. The percentage yield of this carboxylic acid hydrazide was high (Mirfazli, et al., 2014). Besides, the melting point of the carboxylic acid hydrazide was determined too.

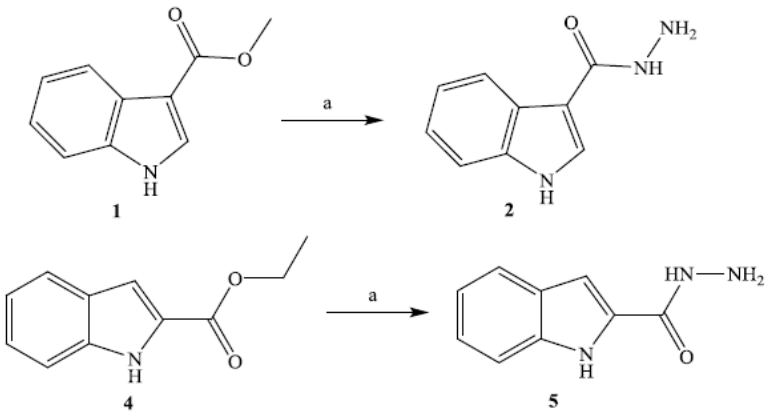

Reagents: a) 99 % hydrazine monohydrate ($NH_2NH_2 \cdot H_2O$), a minimum amount of ethanol.

Reaction condition: Reflux at 80 ℃ for 2 hours.

Scheme 2.5: Synthesis of carboxylic acid hydrazide (Compound 2 and 5) (Mirfazli, et al., 2014)

2.2.2 Green methods

2.2.2.1 Ultrasound Irradiation

In the green synthesis of carboxylic acid hydrazide, ultrasound irradiation is used as the cleaner source of energy. 20 mmol of ethyl 4-aminobenzoate and 8 mL of 99 % hydrazine monohydrate were used as the starting material to produce the final desired product, 4-aminobenzohydrazide. The reaction was carried out under ultrasound irradiation conditions for one hour. Then, the white solid product was obtained through filtration and subjected to recrystallisation from ethanol. The chemical structure of 4-aminobenzohydrazide was confirmed by using FTIR (KBr pellet method), ^{1}H NMR as well as ^{13}C NMR (DMSO-d_6). The advantage of using ultrasound irradiation is that it reduced the required reaction time by accelerating the rate of reaction. Besides that, it also enhanced the amount of product obtained as compared to the classical method used (Younis and Awad, 2020).

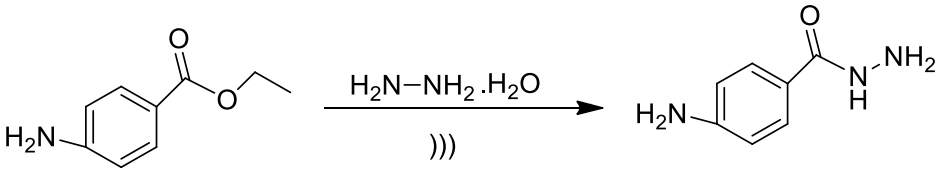

Reaction condition:))) represents ultrasonic radiation

Scheme 2.6: Synthesis of carboxylic acid hydrazide through ultrasound irradiation method (Younis and Awad, 2020)

2.2.2.2 Utilization of ionic liquid

A group of researchers proposed an alternative pathway to synthesise the substituted carboxylic acid hydrazide by using ionic liquid at room temperature. This hydroacylation reaction involved azodicarboxylate and propionaldehyde as the reactants. The ionic liquid used was 1-butyl-3-methylimidazolium as shown in **Figure 2.1**. By using this ionic liquid as the solvent, metal catalysts such as copper, zinc and tungsten, which are hazardous and expensive, are not needed to promote the reaction. Besides, the rate of hydroacylation reaction was enhanced when the temperature of the reaction was increased to 40 ^{o}C (Shamsabadi and Chudasama, 2016).

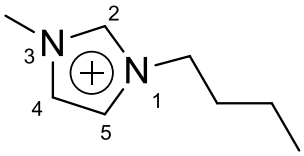

Figure 2.1: Chemical structure of the ionic liquid 1-butyl-3-methylimidazolium [BMIM] cation (Shamsabadi and Chudasama, 2016)

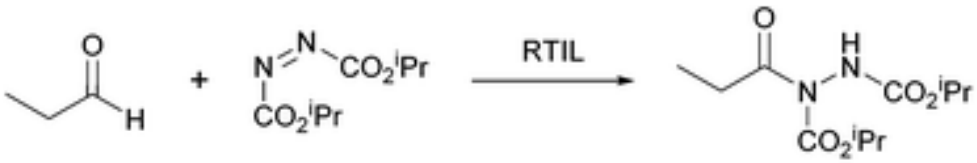

Scheme 2.7: Synthesis of carboxylic acid hydrazide by using ionic liquid (Shamsabadi and Chudasama, 2016)

2.3 Synthesis of *N*-acylhydrazone

N-acylhydrazone can be synthesised through the reaction between a carboxylic hydrazide and an aldehyde group. Usually, aromatic aldehyde will be used while ethanol is the most frequently used solvent. The amino group of the carboxylic hydrazide works as a nucleophile to attack the carbon of the carbonyl group that bears a partial positive charge. As a result, an alkoxide ion formed as an intermediate. After the proton is transferred from nitrogen to the oxygen atom, carbinolamine is produced. Then, the oxygen atom of the carbinolamine accepts another hydrogen atom from (+)-tartaric acid to become a water molecule. This water molecule is a better leaving group than the hydroxyl group as it is stable. The nitrogen atom of the intermediate donated one proton back to (+)-tartaric acid, generating *N*-acylhydrazone. (+)-Tartaric acid is considered a catalyst as it regenerated at the end of the reaction. Organic solvent and reflux systems will normally be involved in this condensation reaction (Zhao, Cheng and Pang, 2018). The progress of the reaction is monitored by using the TLC method. The structure of the chemical compound synthesised will be confirmed by using FTIR, ^{1}H NMR as well as ^{13}C NMR. Besides, the melting point of the *N*-acylhydrazone is determined too.

2.3.1 Conventional method

Acyl hydrazine was condensed with an aromatic aldehyde compound in the presence of acid as the catalyst. This condensation reaction took place at ambient temperature. A high yield of product formed was obtained after 2 hours. A wide variety of *N*-acylhydrazone could be synthesised by changing the alkyl substituents on the acyl hydrazine and also aromatic aldehyde. Besides, alternating the position of the substituents would also generate different *N*-acylhydrazone compounds. It was observed that the meta-substituted aromatic aldehyde (82 - 98 %) gained a higher amount of product than that of the para-substituted aromatic aldehyde (62 - 89 %) (Rodrigues, et al., 2016).

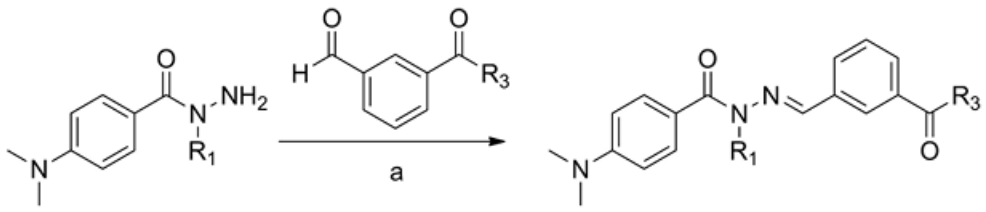

Reagent: a) HCl (as catalyst), ethanol; R_1: H, CH_3; R_3: OH, OCH_3, NHOH

Condition: 2 hours, room temperature, yield (82 - 98 %)

Scheme 2.8: Synthesis of *N*-acylhydrazone using meta substituted aromatic aldehyde (Rodrigues, et al., 2016)

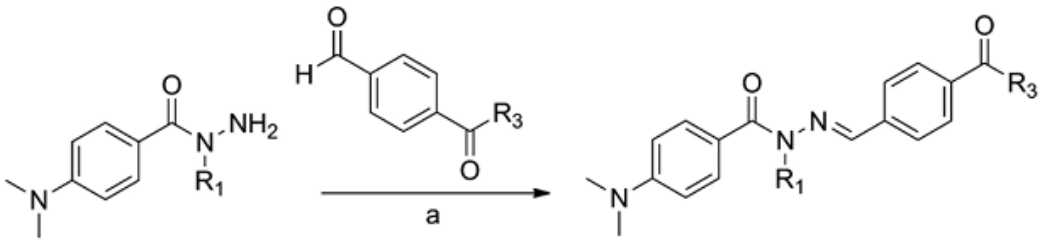

Reagent: a) HCl (as catalyst), ethanol; R_1: H, CH_3; R_3: OH, OCH_3, NHOH

Reaction condition: 2 hours, room temperature, yield (62 - 89 %)

Scheme 2.9: Synthesis of *N*-acylhydrazone using *para*-substituted aromatic aldehyde (Rodrigues, et al., 2016)

Furthermore, another group of researchers proposed a more complicated pathway to synthesise *N*-acylhydrazone. It involved a total of 5 steps. The aromatic aldehyde or more specifically vanillic aldehyde was first undergoing reduction to produce primary alcohol in the presence of water and activated carbon in tetrahydrofuran, THF. The reducing agent used is sodium borohydride, $NaBH_4$. Then, the primary alcohol was converted to azide due to the reaction with thionyl chloride, $SOCl_2$ in dichloromethane, DMF. Then, the azide intermediate was reacted with ethyl propiolate to produce triazole ester. This ester was converted to hydrazide with the help of hydrazine monohydrate. The important intermediate of hydrazide then reacted with the aldehyde group to produce the final desired product, *N*-acylhydrazone (Silva, et al., 2020).

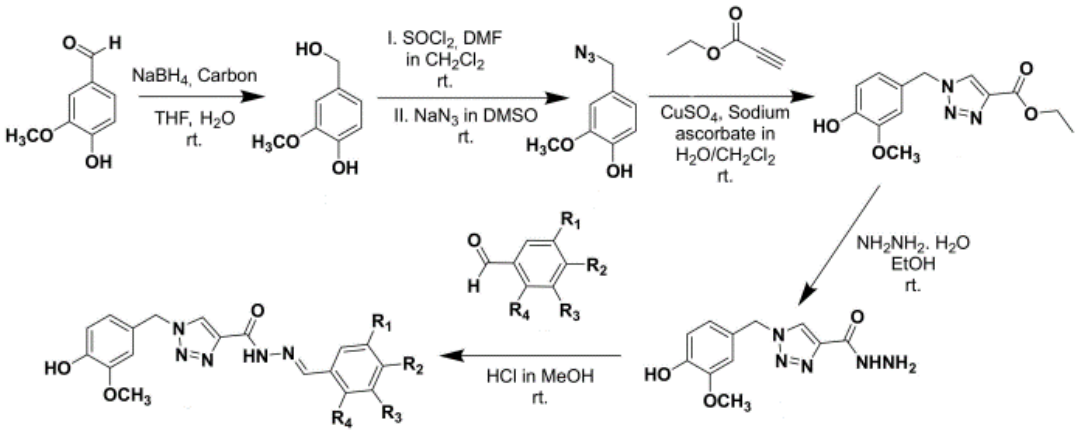

Scheme 2.10: Complex synthesis pathway of *N*-acylhydrazone (Silva, et al., 2020)

Apart from that, an equal molar (0.36 mmol) of pyrimidine-2-carbohydrazide and different types of heteroaromatic or aromatic aldehyde was utilised as the starting material to synthesise *N*-acylhydrazone. The solid product, 2-pyrimidinyl-*N*-acylhydrazone and its derivatives obtained were washed with a minimum amount of cold diethyl ether. The percentage yields of the products were recorded between 40 to 88 %. The chemical structure of the compounds synthesised was elucidated by using NMR (Coimbra, et al., 2019).

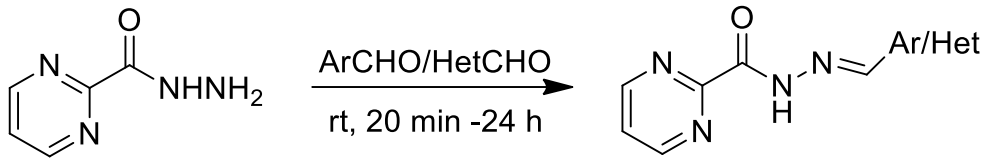

Reagent: Aromatic aldehyde/heteroaromatic aldehyde, ethanol

Reaction condition: Room temperature, stirring for 20 minutes to 24 hours.

Scheme 2.11: Synthesis of 2-pyrimidinyl-*N*-acylhydrazone and its derivatives (Coimbra, et al., 2019)

Moreover, coumarin-based *N*-acylhydrazone was generated through the reaction between 3-acetyl-7-hydroxy-2*H*-chromen-2-one, a heteroaromatic aldehyde and benzohydrazide. The final product of this condensation reaction is *N*-acylhydrazone which will function as the coumarin dye. The solvent used was ethanol and acetic acid played an important role as the catalyst in this reaction. The completion of the reaction was determined by using the TLC method. It was found that the reactants were fully consumed only after 24 hours. Hence, the researchers proposed an improved method for this reaction and it will be further discussed in **Section 2.3.2.1** (Pereira, et al., 2016).

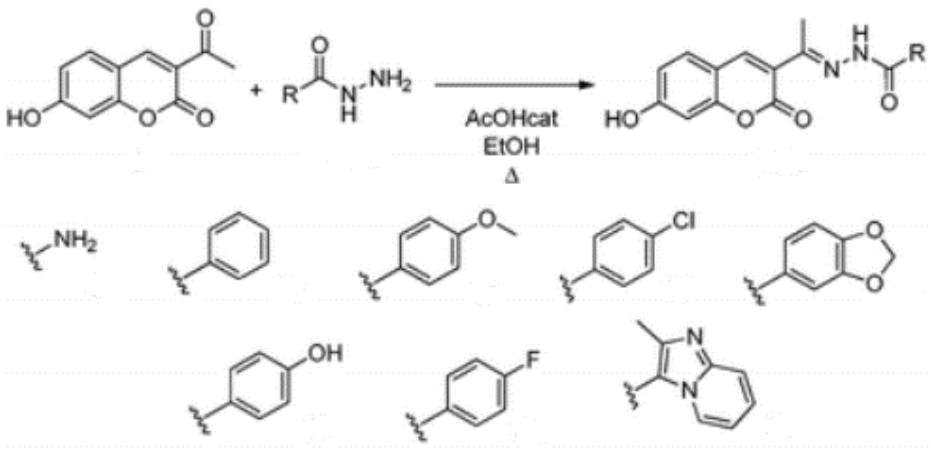

Scheme 2.12: Synthesis of coumarin-based *N*-acylhydrazone and its derivatives (Pereira, et al., 2016)

2.3.2 Green Methods

2.3.2.1 Microwave-assisted reaction

In the improved method, 3-acetyl-7-hydroxy-2*H*-chromen-2-one, a heteroaromatic aldehyde and different types of benzohydrazide were reacted under microwave irradiation. The usage of microwave irradiation greatly reduced the time required for the completion of reaction, from 24 hours to 1 hour. Furthermore, some of the reactions resulted a greater percentage yield as compared to the classical method. The temperature of this green reaction was set at 80 ^{o}C. It was found that the elevation of temperature to 100 ^{o}C would not enhance the rate of reaction. However, the condensation reaction that occurred at 150 ^{o}C was prohibited as it led to the degradation of the products (Pereira, et al., 2016).

Table 2.1: Comparison done between the conventional method and microwave assisted method (Pereira, et al., 2016).

Products	**Conventional heating**			**Microwave**		
	Time	Temp. (^{o}C)	Yield (%)	Time	Temp. (^{o}C)	Yield (%)
3a	20 h	80	88	45 min	80	93
3b	24 h	80	69	1 h	80/100	Nd
3b	-	-	-	1 h	150	Nd
3b	-	-	-	1 h	80	89
3b	24 h	80	71	-	-	
3c	24 h	80	78	1 h	80	95
3d	24 h	80	87	1 h	80	98
3e	24 h	80	82	1 h	80	93
3f	24 h	80	70	1 h	80	97
3g	24 h	80	83	1 h	80	74
3g	-	-	-	1.5 h	80	85
3h	24 h	80	72	1 h	80	82

*Nd represents not determined.

2.3.2.2. Grinding technique

This group of researchers used benzohydrazide and various types of aromatic carbonyl compounds as the starting materials. Besides, a minimum volume of acetic acid was utilised as the catalyst in this reaction. The reactants were ground for 10 minutes at room temperature. The grinding process provided the energy required to initiate the chemical reaction. The grinding process had replaced the conventional heating source. Furthermore, the researchers also determined the appropriate ratio of acetic acid and water in order to maximise the rate of reaction. Water played an essential role in this reaction to produce a slurry mixture. Thus, a lesser amount of catalyst could be added which would then produce a homogenised reaction mixture. During the grinding process, the reaction mixture would become dry as a result of the evaporation process. Thus, more acetic acid and water mixture had to be added. Additionally, acetic acid had been proven to have an effective catalytic reaction in this synthesis. This situation happened because the reaction that was carried out without acetic acid (only water alone) took 1.3 hours to be achieved while that involved acetic acid/water mixture only required 2 minutes. Thus, the presence of acetic acid greatly enhanced the rate of the condensation reaction. Besides, the ideal ratio of acetic acid/water was found to be 1:2 (Filho and Pinheiro, 2017).

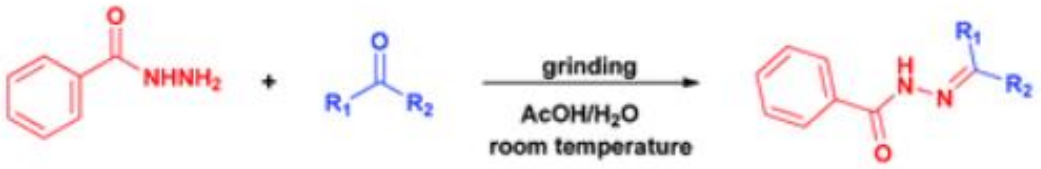

Scheme 2.13: Synthesis of *N*-acylhydrazone using a grinding technique (Filho and Pinheiro, 2017)

2.4 Conformational study of *N*-acylhydrazone and its derivatives

Fourier Transform Infrared Spectroscopy (FTIR) managed to provide information such as the functional groups that are present in the compound. However, it is unable to determine the real structure of the compound. Hence, additional confirmation analysis is normally needed to acquire additional and detailed information about the structure of the compounds. Conformational study on *N*-acylhydrazone is normally required as it contains both imine and amide functional groups that will give rise to different stereoisomers. The analysis is normally done by using 1D-NMR and 2D-NMR.

2.4.1 Determination of the relative configuration of the imine double bond

The nature of the substituents attached to the imine functional group (HC=N) might lead to different *E/Z* isomers equilibrium. For instance, the size of the substituents affected the *E/Z* configuration. The substituents with bigger sizes would generate steric hindrance on the imine bond. Hence, the steric hindrance would cause most of the *N*-acylhydrazone to exist in *(E)* configuration. Besides that, it was found that the types of the NMR solvent used would influence the *E/Z* configuration too. For instance, the isomeric ratio of the *E/Z* stereoisomers of *N*-acylhydrazone reduced by 10 % when $CDCl_3$ replaced DMSO-d_6 as the solvent used in the 2D-NMR. When $CDCl_3$ is used, the -NH signal of the *(Z)* stereoisomers could be found at higher chemical shifts. This situation happened because the stereoisomer was stabilised by the intramolecular hydrogen bonding with the deuterated $CDCl_3$ solvent (Tiem and Morjan, 2020).

A differential Nuclear Overhauser Effect (NOE) experiment was carried out to investigate the structure proximity of the compounds. The proton of imine bond was irradiated and an intensified signal was observed at the proton that was able to couple with HC=N. From this experiment, it was concluded that *(E)* form of *N*-acylhydrazone was found. For example, the irradiation of the proton at δ 11.57 (CO-NH) led to a 12 % and 20 % of NOE Enhancement on the proton at δ 8.44 (aromatic H) and δ 7.80 (N=CH) respectively (Rodrigues, et al., 2016). If the compound is present in *(Z)* stereoisomer, the proton of the imine bond might not be able to interact with the proton of CO-NH.

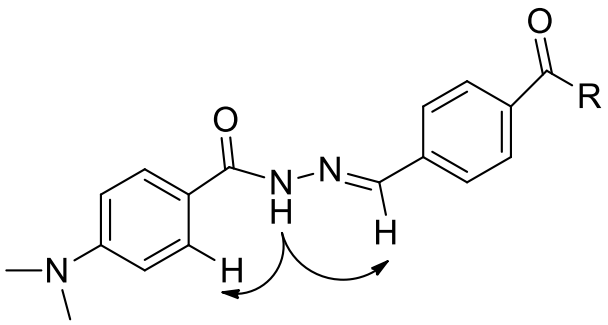

Figure 2.3: Chemical structure of *N*-acylhydrazone that undergo NOE experiment

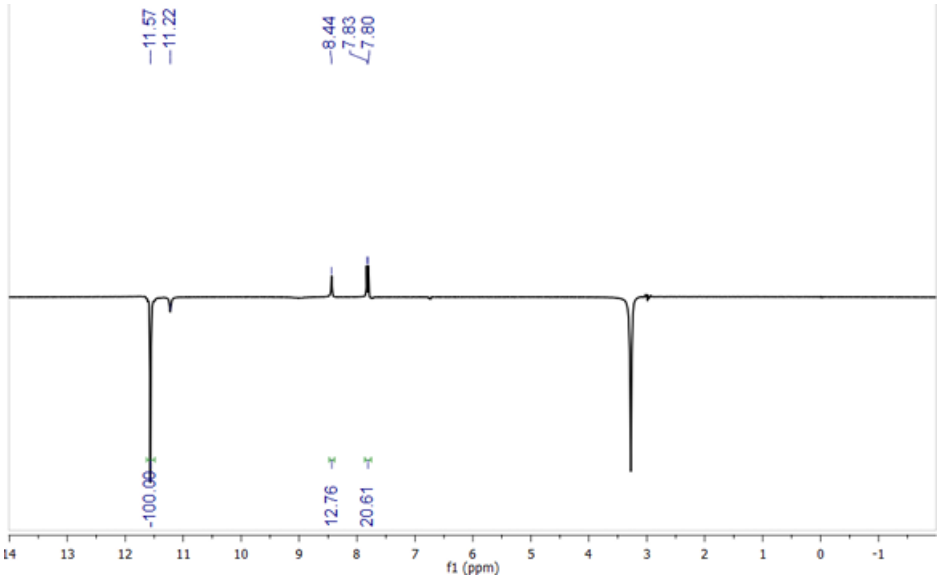

Figure 2.4: NOE spectrum of *N*-acylhydrazone synthesised (irradiation at δ 11.57 ppm) (Rodrigues, et al., 2016)

2.4.2 CO-NH rotational barrier

Besides *E/Z* configuration, *N*-acylhydrazone can also exist in *cis* or *trans* conformers about the amide, CO-NH bond. This situation happened due to the inversion of the amide bond. The different spatial structures of *N*-acylhydrazone were shown in **Figure 2.5**. The presence of the *cis* or *trans* conformers was confirmed by the two broad singlets peak that was found at the chemical shift of 12.10 to 11.77 ppm in the ^{1}H NMR spectrum as shown in Appendix A (Aarjane, Slassi and Amine, 2020).

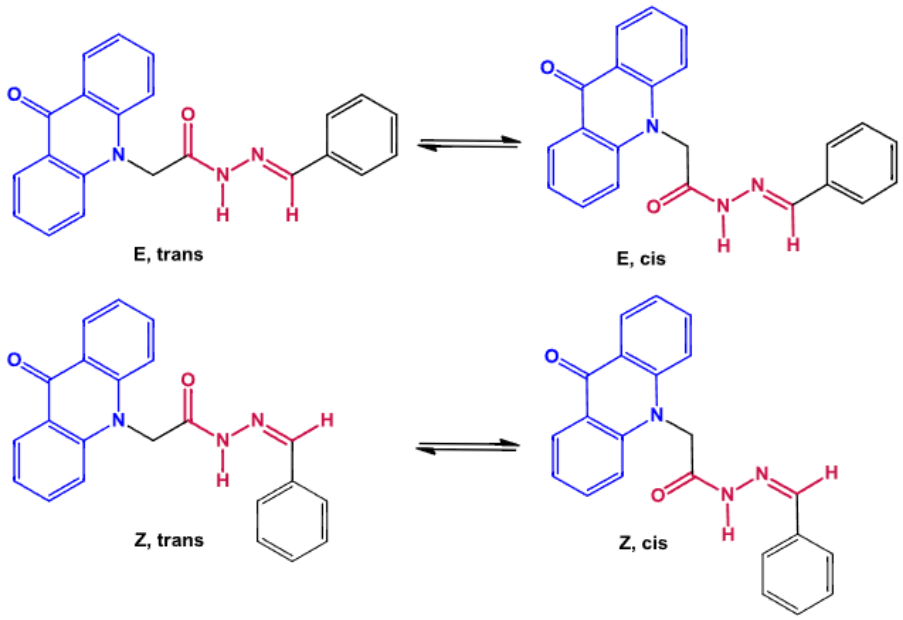

Figure 2.5: *E/Z* and *cis/trans* isomers of *N*-acylhydrazone (Aarjane, Slassi and Amine, 2020).

Dynamic NMR experiment was also used to determine the conformational of products synthesised by using DMSO-d_6 as the solvent. This experiment determines the exchange rate constant of the *cis* and *trans* rotamers as well as the energy of the rotational barrier of the compounds. According to **Figure 2.6**, two broad singlet peaks can be observed at 298 K. These two peaks were all belong to the proton of the amide group which resulted from the *cis*/*trans* conformers. As the temperature increased, the two peaks became closer, broaden and finally combined when the temperature reached 348 K. Thus, the coalescence temperature, T_c which is the temperature at which the two singlet peaks of amide bond combined to become one peak was determined to be 348 K. At this temperature, the exchange rate of the *cis*/*trans* rotamers are identical and hence, NMR was unable to distinguish the signal between them and so seeing them as one peak. Then, the Gibbs free energy of activation or the energy for the rotational barrier can be figured out by using the Gutowsky equation ($k_c = \frac{\pi\Delta\nu}{\sqrt{2}}$) as well as the Eyring equation ($\Delta G^{\neq}$ = 19.14 T_c (10.32 + $\log\frac{T_c}{k_c}$)$\times 10^{-3}$). The energy of the rotational barrier is defined as the energy needed to initiate a rotation around a bond. The higher $\Delta G^{\neq}$ value indicates more energy is required to overcome the barrier and cause rotation around the bond (Aarjane, Slassi and Amine, 2020). High-Performance Liquid Chromatography (HPLC) was not used in this case as it is unable to detect the fast exchange between the *cis* and *trans* rotamers (Tiem and Morjan, 2020).

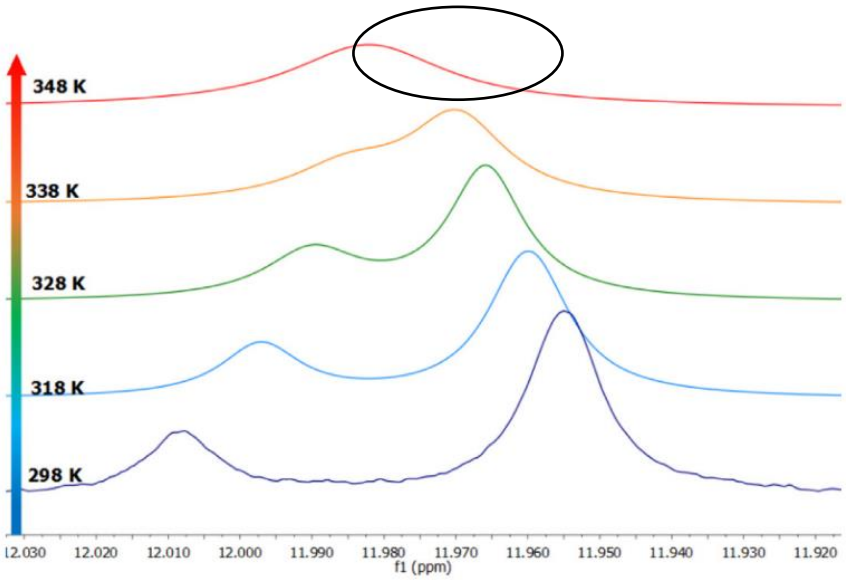

Figure 2.6: ^{1}H NMR spectrum of proton of CO-NH bond at various temperatures (Aarjane, Slassi and Amine, 2020)

2.5 Antibacterial activity of *N*-acylhydrazone and its derivatives

Several methods can be used to evaluate the antibacterial activity of the compounds produced. For example, diffusion, dilution and TLC methods can be used for screening the activity. Among these, the dilution method or more specifically broth dilution method was used as it is fast, convenient and able to provide qualitative and quantitative information. The existence of antibacterial activity can be determined by observing the colour. Besides, the minimum inhibitory concentration (MIC) value of the compound can be determined too.

2.5.1 Determination of minimum inhibitory concentration (MIC)

Broth dilution methods followed the protocols of Clinical and Laboratory Standards Institute (CLSI). Besides, it requires serial dilution or more specifically two-fold dilution for the compounds or antibacterial agent.

A group of researchers introduced acylhydrazone group into the acridone group in order to generate new *N*-acylhydrazone compounds that might have antibacterial activity. This situation happened because more bacteria had developed resistance to the existing acridone-based drug. The MIC values of the newly synthesised compounds were determined and the bacteria strain chosen for studies included *Staphylococcus aureus* (Gram-positive), *Escherichia coli*, *Pseudomonas putida* and *Klebsiella pneumonia* (Gram-negative). It was concluded that the newly synthesised acridone-based *N*-acylhydrazone compounds could inhibit the visible growth of *Staphylococcus aureus* effectively. The nature and presence of substituents would affect the antibacterial activity of the compounds. Besides, the compound with para-dimethylamino substituted on the benzene ring exhibited the strongest antibacterial activity against *Pseudomonas putida* and obtained a MIC value of 38.46 μg/mL as compared to chloramphenicol (an antibiotic) that has a MIC value of 37.03 μg/mL. The nature and presence of substituents would affect the antibacterial activity of the compounds (Aarjane, et al., 2020).

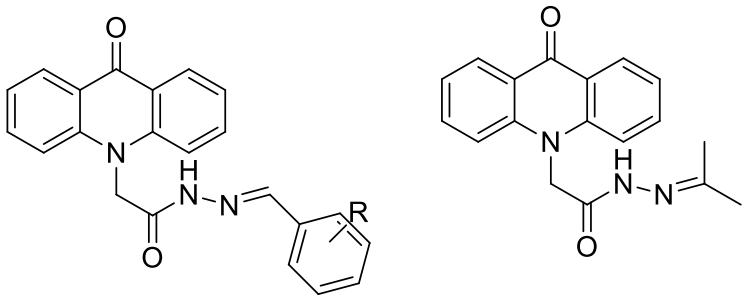

Figure 2.7: Chemical structure of the acridone based *N*-acylhydrazone (Aarjane, et al., 2020)

CHAPTER 3

MATERIALS AND METHODOLOGY

3.1 Chemicals used

Table 3.1: Chemicals used in the synthesis of ester

Chemical name **Molecular formula**	**Molecular weight, g mol^{-1}**	**State**	**Manufacturer** **Country**
Acetic acid CH_3COOH	60.05	Liquid	Merck, Germany
Absolute ethanol C_2H_5OH	46.07	Liquid	Fisher Scientific, Malaysia
Concentrated hydrochloric acid HCl	36.46	Liquid	Fisher Scientific, UK
Ethyl acetate $C_4H_8O_2$	88.11	Liquid	LAB-SCAN, Ireland
Sodium sulphate anhydrous Na_2SO_4	142.04	Solid	Merck, Germany

Table 3.2: Chemicals used in the synthesis of carboxylic acid hydrazide

Chemical name **Molecular formula**	**Molecular weight, g mol^{-1}**	**State**	**Manufacturer** **Country**
Hydrazine hydrate $NH_2NH_2{\cdot}H_2O$	50.06	Liquid	Merck, Germany
Absolute ethanol C_2H_5OH	46.07	Liquid	Fisher Scientific, Malaysia
Ethyl acetate $C_4H_8O_2$	88.11	Liquid	LAB-SCAN, Ireland

Table 3.3: Chemicals used in the synthesis of *N*-acylhydrazone

Chemical name **Molecular formula**	**Molecular weight,**	**State**	**Manufacturer** **Country**

	g mol^{-1}		
Benzaldehyde C_7H_6O	106.12	Liquid	R&M marketing, UK
2-Hydroxybenzaldehyde $C_7H_6O_2$	122.12	Liquid	Merck, Germany
4-Hydroxybenzaldehyde $C_7H_6O_2$	122.12	Solid	Merck, Germany
2-Chlorobenzaldehyde C_7H_5ClO	140.57	Liquid	Merck, Germany
4-Chlorobenzaldehyde C_7H_5ClO	140.57	Liquid	Merck, Germany
2,4-Dichlorobenzaldehyde $C_7H_4Cl_2O$	175.01	Solid	Merck, Germany
3,4-Dichlorobenzaldehyde $C_7H_4Cl_2O$	175.01	Solid	Acros Organics, Belgium
4-Fluorobenzaldehyde C_7H_5FO	124.11	Liquid	Merck, Germany
4-Methylbenzaldehyde C_8H_8O	120.15	Liquid	Merck, Germany
4-Dimethylaminobenzaldehyde $C_9H_{11}NO$	149.19	Solid	Merck, Germany
Tartaric acid $C_4H_6O_6$	150.09	Solid	Fisher Scientific, UK
Absolute ethanol C_2H_5OH	46.07	Liquid	Fisher Scientific, Malaysia

Table 3.4: Chemicals used in Thin Layer Chromatography

Chemical name Molecular formula	Molecular weight, g mol^{-1}	State	Manufacturer Country
Chloroform $CHCl_3$	119.38	Liquid	Merck, Germany
Ethyl acetate $C_4H_8O_2$	88.11	Liquid	LAB-SCAN, Ireland
n-Hexane C_6H_{14}	86.18	Liquid	Merck, Germany
Ethanol C_2H_5OH	46.07	Liquid	Fisher Scientific, Malaysia

Table 3.5: Chemicals used in recrystallisation

Chemical name Molecular formula	Molecular weight,	State	Manufacturer Country

	g mol^{-1}		
Ethanol C_2H_5OH	46.07	Liquid	Fisher Scientific, Malaysia

Table 3.6: Chemicals used in FT-IR and NMR spectroscopies

Chemical name Molecular formula	Molecular weight, g mol^{-1}	State	Manufacturer Country
Dimethyl sulfoxide-d6 C_2D_6OS	84.17	Liquid	Fisher Scientific, UK
Potassium Bromide KBr	119.00	Solid	Sigma-Aldrich, USA

Table 3.7: Chemicals used in antibacterial activity analysis

Chemical name Molecular formula	**Molecular weight, g mol^{-1}**	**State**	**Manufacturer Country**
Ethanol C_2H_5OH	46.07	Liquid	Fisher Scientific, Malaysia
p-iodonitrotetrazolium chloride $C_{19}H_{13}ClN_5O_2$	505.7	Solid	MP Biomedical, Germany
Streptomycin sulfate, *Streptomycin sp.*	1457.7	Solid	Merck, Germany

3.2 Instrumentation

Table 3.8: Instruments used in the project

Instrumentation	Manufacturer, Model
FT-IR Spectrophotometer	Perkin Elmer, Spectrum RX1
Rotary Evaporator	BUCHI, Rotavapor R-200 Heating Bath B-491
Sonicator	Elmasonic, S 100 H
Melting point apparatus	Stuart, SMP10
Nuclear Magnetic Resonance Spectrometer	JEOL, JNM-ECX400
Incubator	Memmert, Germany
Lamina air flow cabinet	ESCO, USA
UV/Vis Spectrophotometer	Thermo Scientific, Germany

3.3 Experimental Procedure

The chemicals used in the final year project were listed in **Table 3.1** to **Table 3.3** according to the intermediate produced. The glassware and apparatus used were a separating funnel, filter funnel, beakers, conical flask, measuring cylinder, thermometer (alcohol and mercury typed), reflux condenser, Buchner funnel, glass rod, dropper and bulb, oil bath, hot plate magnetic stirrer and vacuum pump.

3.3.1 Synthesis of ester

The starting materials of this project are hydrochloride and ester. Firstly, these two chemicals were weighed or measured and transferred into a clean 250 mL round bottom flask. Then, 70 mL of acetic acid that acted as the solvent was added to the mixture. A magnetic stir bar and a small amount of boiling chips were also added to the 250 mL round bottom flask. The reaction mixture was then allowed to reflux in an oil bath at 80 ^{o}C for 6 hours. The pipes were connected to allow the water to flow in from the bottom and flow out through the top part of the condenser. This anti-gravity process was to ensure that the cold water can always fill the condenser and provide the cooling effect effectively to the reflux system. Thin Layer Chromatography was used to monitor the progress of the chemical reaction in order to determine the completion of the reaction.

Once the reaction was completed, the reaction mixture was cooled down and then transferred into a beaker filled with 300 mL of ice water. After that, 40 mL of ethyl acetate was used to extract desired compounds into the organic layer. The bottom aqueous layer was dispensed back into the beaker and the extraction was repeated another two times. On the other hand, the upper organic layer was collected in another new beaker. Anhydrous sodium sulphate was added to the beaker to absorb moisture in the organic layer. When anhydrous sodium sulphate powder could move freely in the beaker, this indicated that the organic layer was dried. The dried organic layer was concentrated under reduced pressure using a rotary evaporator. The round bottom flask with concentrated extract was covered with aluminium foil.

3.3.2 Synthesis of carboxylic acid hydrazide

On the following day, 50 mmol of ester and 150 mmol of 99% hydrazine hydrate (7.28 mL) were added into a clean 250 mL round bottom flask. Then, 25 mL of absolute ethanol was added to the round bottom flask. The reaction mixture was allowed to sonicate in order to dissolve all reactants. A magnetic stir bar and a small amount of boiling chips were added to the reaction mixture. It was then refluxed in an oil bath at 80 ^{o}C for six hours. Thin Layer Chromatography was again utilised to monitor the progress of the reaction. Once the reaction is completed, the reaction mixture was cooled down to room temperature and then transferred into a beaker filled with 300 mL of ice water. Extraction was done a total of three times by using 40 mL of ethyl acetate each. The collected organic layer was added with anhydrous sodium sulphate, which is a drying agent. The solvent in the organic layer was evaporated under reduced pressure by using a rotary evaporator. It was then purified by recrystallisation in 95% of hot ethanol. The round bottom flask with the crude product inside was covered with aluminium foil.

3.3.3 Synthesis of *N*-acylhydrazones SB 1 – SB 10

A series of *N*-acylhydrazone and its derivatives were synthesised by refluxing the carboxylic acid hydrazide with various types of benzaldehydes as listed in **Table 3.9**.

Table 3.9: Various benzaldehydes used in the synthesis of *N*-acylhydrazones

Benzaldehyde	Molecular weight, g mol^{-1}	2 mmol	
		Mass (g)	Volume (µL)
Benzaldehyde	106.12	-	203
2-Hydroxybenzaldehyde	122.12	-	214
4-Hydroxybenzaldehyde	122.12	0.2442	-
2-Chlorobenzaldehyde	140.57	-	226
4-Chlorobenzaldehyde	140.57	-	234
2,4-Dichlorobenzaldehyde	175.01	0.3500	-
3,4-Dichlorobenzaldehyde	175.01	0.3500	-
4-Fluorobenzaldehyde	124.11	-	215
4-Methylbenzaldehyde	120.15	-	236
4-Dimethylaminobenzaldehyde	177.24	0.3545	-

Mass of reagent needed, g

= Number of moles (mol) x Molecular weight (g mol^{-1})

Volume of reagent needed, mL = $\frac{\text{Mass of reagent used (mol)}}{\text{Molecular weight (g mol}-1)}$

2.0 mmol (0.5250 g) of the crude product carboxylic acid hydrazide and 2.0 mmol of benzaldehyde were added into a 50 mL round bottom flask. Then, 0.25 g of acid which functioned as the catalyst was also added to it, followed by 15 mL of absolute ethanol. The reaction mixture was allowed to sonicate in order to dissolve all the reactants. A magnetic stir bar and a small amount of boiling chips were added to the reaction mixture. The mixture was subjected to reflux in an oil bath at 80 ^{o}C for 8 hours. The progress of the chemical reaction is monitored by using Thin Layer Chromatography. After the chemical reaction has completed, the reaction mixture was cooled to room temperature

and then transferred into a beaker that contained approximately 10 g of crushed ice. The crude product (*N*-acylhydrazone) produced was filtered by using vacuum filtration. The product was washed with cold distilled water in order to remove the acid.

3.3.4 Purification by recrystallisation

The crude product obtained was purified by recrystallisation by dissolving it in a minimum amount of hot 95% of ethanol. The solution was filtered to remove the insoluble impurities likewise dust and filter paper fibre. The filtration apparatus was preheated in order to prevent some of the product from precipitating from the solution. Besides, the filtrate was collected in a conical flask that was filled with a small volume of boiling ethanol. These steps ensured that the filtration apparatus was warm by the hot ethanol vapour. This situation happened as the crystallisation of product from the solution would cause the loss in product and thus decrease the percentage yield. After filtration, a small volume of hot ethanol was used to rinse the glass rod, beakers and cotton wool to maximise the yield of the product.

The filtrate collected in the conical flask was heated to $\frac{1}{3}$ of its original volume. Then, the saturated solution was allowed to cool to room temperature in order

to promote crystallisation. The crystallized product was washed with a minimum volume of ethanol and dried in the oven.

3.4 Characterisation of the Products Synthesised

3.4.1 Thin Layer Chromatography (TLC)

TLC method was used to monitor the progress of the reaction and to determine the purity of the product. A small amount (~0.5 mL) of the reaction mixture or product was transferred into a clean sample vial. Then, a minimum volume of ethanol followed by chloroform was added to dissolve the compound. An adequate amount of the sample solution was spotted on the baseline drawn on the TLC plate by using a capillary tube. The spots were at least 0.5 cm away from one another to prevent the overlapping of the compounds.

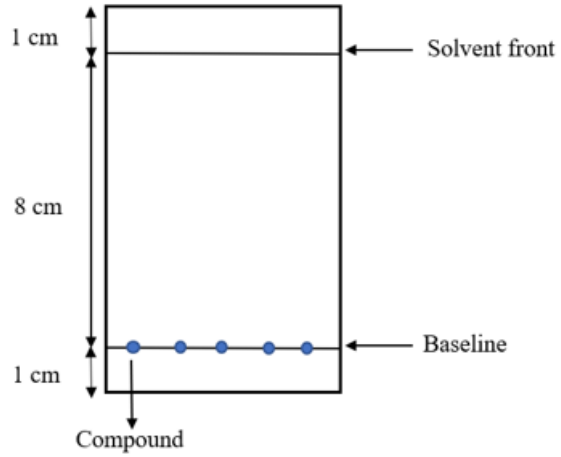

Figure 3.1: Outline of Thin Layer Chromatography

The plate was then developed with a mixture of a 1:1 ratio of *n*-hexane and ethyl acetate. When the solvent front moved approximately 1 cm from the top

of the TLC plate, the plate was removed from the developed chamber. The mobile phase was allowed to evaporate and the TLC plate was visualised under an ultraviolet lamp with a short wavelength (254 nm). This also indicated that the compounds synthesised consist of conjugated and aromatic ring. The spots on the plate were marked with a pencil. The retention factor, R_f value for each compound were calculated by using the formula shown below.

$$R_f = \frac{D}{L}$$

Where, D = Distance travelled by sample from the baseline

L = Distance travelled by solvent from the baseline

3.4.2 Melting Point

The melting points of all the compounds synthesised were observed by using melting point apparatus. The melting point represented the purity of the compound. The wide range of melting points indicated the low purity of the compounds while the pure compounds had a narrower range of melting points.

A haematocrit capillary tube was used and a small amount of solid samples were inserted into it. Then, the tube was then placed into a melting point apparatus with the temperature set around 200 ^{o}C. The melting point range of each sample was recorded from the temperature at which the sample started to

melt to the temperature at which the sample totally melted. The melting point of each compound was observed twice in order to obtain an accurate result.

3.4.3 Fourier Transform Infrared Spectroscopy (FT-IR)

FTIR was utilised to identify the functional groups that are present in the compounds produced. The determination of the functional groups was done by observing the significant peaks at a certain frequency range. This situation happened as different chemical bonds will vibrate at different frequencies and thus were detected at different wavenumber. There are various unique absorptions which allow the specific functional group to be determined. The molecular structure of the compound was then elucidated by referring to the standard IR spectrum table.

A small amount of the solid compound synthesised was mixed with anhydrous potassium bromide (KBr) in the ratio of 1:10. KBr allows the 100% transmittance of the infrared radiation and thus will not interfere with the result. Hence, the KBR must be kept in the oven when not in use to prevent the KBr from absorbing water from the surrounding. Water molecules will contaminate the KBr salt and interfere with the spectrum. The mixture of compound and KBr salt was ground by using an agate mortar and pestle into fine powder. The fine powder was compressed into a KBr pellet by using a hydraulic pressure press. The KBr pellet was then analysed by using FTIR and scanned at infrared radiation from 4000 cm^{-1} to 400 cm^{-1}.

3.4.4 Nuclear Magnetic Resonance (NMR) Spectroscopy

NMR was used to elucidate the structure of the compounds synthesised. There are two types of NMR experiments which are ^{1}H NMR as well as ^{13}C NMR. NMR works based on the magnetic property of the nucleus of the atom. NMR provides qualitative and quantitative information likewise the types and the number of the proton or carbon present in the compound's structure. Besides, the methyl, methylene and methine proton could be differentiated by using Distortionless Enhancement by Polarisation Transfer (DEPT) NMR. The connection between the molecules could be determined through the help of Heteronuclear Multiple Quantum Coherence (HMQC) and also Heteronuclear Multiple Bond Correlation (HMBC).

For the sample preparation, approximately 20 mg of the compound synthesised was weighed in a clean sample vial and dissolved in a minimum amount of DMSO-d_6. The dissolved sample solution was transferred into an NMR tube to a height of about 4 cm. The tube was labelled and analysed by using NMR spectrometer.

3.5 Conformational Study of *N*-acylhydrazone and its derivatives

3.5.1 Determination of the relative configuration of the imine double bond

N-acylhydrazone can be found in four possible forms which are *cis*-amide/$E_{C=N}$, *trans*-amide/$E_{C=N}$, *cis*-amide/$Z_{C=N}$, *trans*-amide/$Z_{C=N}$. The *cis/trans* rotamers

are due to the inversion of the CO-NH bond while the *E/Z* configurations are the effect found at the HC=N bond. The configuration of compounds synthesised can be determined through Differential Nuclear Overhauser Effect (differential NOE) experiment (2D-NMR). Differential NOE managed to differentiate protons by their spatial location in the structure of the compounds. It helps to visualise the 3D molecular structure of *N*-acylhydrazones. For instance, the proton of the amide group was irradiated. As there are two types of singlet signals peak found, the one at the lower chemical shift and with higher intensity was chosen in this case. Any other protons that close and interact with the proton of the amide group would experience an enhancement in the signal intensity. Through this experiment, the *E/Z* geometrical isomers could be determined. The presence of two types of signals in ^{1}H NMR was due to the presence of the *cis/trans* amide rotamers of *N*-acylhydrazones. Besides, the ratio of the *cis/trans* rotamers were determined from the integrations of the amide signal in the ^{1}H NMR spectrum (Aarjane, Slassi and Amine, 2020).

3.5.2 Rotational barriers around the CO-NH (amide) bond of *N*-acylhydrazones

The coalescence temperature (T_c), the exchange rate constant of the *cis/trans* rotamers, (k_c) and also the Gibbs free energy for activation or the energy for the rotational barrier ($\Delta G^{\neq}$) were calculated from the dynamic NMR experiment. The temperature of the analysis increased gradually from 296.15 K to 373.15 K. The temperature where two signals of the proton of the amide bond coalescence was observed and recorded. The value of k_c was calculated

by using the Gutowsky equation, $k_c = \frac{\pi \Delta v}{\sqrt{2}}$, where Δv represents the separation between two singlet peaks in Hertz. Moreover, $\Delta G^{\neq}$ (k$J\ mol^{-1}$) was then figured out by using the Eyring equation, $\Delta G^{\neq}$ = 19.14 T_c (10.32 + log$\frac{T_c}{k_c}$)× 10^{-3} (Aarjane, Slassi and Amine, 2020).

3.6 Antibacterial evaluation on *N*-acylhydrazone and its derivatives

The antibacterial activity of *N*-acylhydrazone and its derivatives synthesised were evaluated by using the broth dilution method (microdilution). There are a total of three bacteria involved which include two Gram-positive bacteria which are *Bacillus subtilis* (BS) (ATCC 6633) and *Staphylococcus aureus* (SA) (ATCC 6538) as well as one Gram-negative bacteria which is *Pseudomonas aeruginosa* (PA) (ATCC 27853). All strains of the bacteria were purchased from the American Type Culture Collection (ATCC). The minimum inhibitory concentration (MIC) values were determined for each compound produced.

3.6.1 Preparation of antibacterial assay

3.6.1.1 Preparation of *N*-acylhydrazone and its derivatives

One mg/mL of the compound synthesised was prepared by dissolving 1 mg of the compound into a labelled and clean sample vial filled with 1 mL of dimethyl sulfoxide (DMSO). The solution was mixed well to ensure the compound is fully dissolved.

3.6.1.2 Preparation of media

Muller-Hinton (MH) agar was prepared by dissolving 15.2 g of the agar powder into a Schott bottle filled with 400 mL of distilled water. Besides, MH broth was prepared by dissolving 8.4 g of powder in another Schott bottle filled with 80 mL of distilled water. The media were then autoclaved. After autoclaved, the MH broth was sealed with parafilm and kept at room temperature. Besides, the MH agar media was poured into a clean petri dish and was allowed to cool. After the agar media was completely solidified, the lid of the petri dish was sealed with parafilm to avoid contamination.

3.6.1.3 Preparation of the bacterial glycerol stock solution

Each of the bacteria was isolated from 50 % of the glycerol stock solution and was streaked on the MH agar plate prepared in section **3.6.1.2** by using an inoculating loop. Then, the agar plate was incubated overnight at 37 ^{o}C. The bacteria colonies were observed on the next day and were used to prepare the bacteria suspension. The bacteria were subcultured to new agar plates weekly.

3.6.1.4 Preparation of standard drug (positive control)

Streptomycin served as a positive control in this antibacterial assay. 100 μg/mL of streptomycin was prepared by dissolving 1 mg of streptomycin in a centrifuge tube filled with 10 mL of sterile distilled water. The centrifuge tube was covered with aluminium foil. The solution was then mixed well and kept in a 4 ^{o}C chiller.

3.6.1.5 Preparation of *p*-iodonitrotetrazolium chloride (INT)

p-iodonitrotetrazolium chloride functioned as the indicator in this antibacterial assay. 0.4 mg/mL of INT was prepared by dissolving 2.0 mg of *p*-iodonitrotetrazolium chloride in a centrifuge tube filled with 5 mL of sterile distilled water and a few drops of concentrated ethanol. The centrifuge tube was covered with aluminium foil as INT is sensitive to light. The solution was then mixed well and kept in a 4 ^{o}C chiller.

3.6.1.6 Preparation of bacteria suspension

Five mL of MH broth was first added into a clean centrifuge tube. Then, the freshly grown bacteria colonies from the agar plate were inoculated into the centrifuge tube by using an inoculating loop. The mixture in the tube was homogenised and 1 mL of the mixture was transferred to a clean cuvette. The absorbance of the mixture was measured at 625 nm by using UV-Visible Spectrophotometer. 625 nm was used as this wavelength is non-destructive to

the cell. The blank used was 1 mL of MH broth solution. The accepted absorbance range was from 0.08 to 0.10 where the turbidity was equivalent to 1 x 10^8 colony forming per unit, cfu/mL (Clinical and Laboratory Standards, 2017).

Once the desired absorbance was obtained, 50 μL of the mixture was transferred into a new centrifuge tube containing 4950 μL of MH Broth. The solution was homogenised and 1 x 10^6 cfu/mL of bacteria suspension was produced.

3.6.2 Determination of Minimum Inhibitory Concentration (MIC) value by using broth dilution method.

The broth dilution method (microdilution method) was used in this study to determine the minimum inhibitory concentration (MIC) value for each compound synthesised against the three types of bacteria. All the procedure was done by using a 96-well plate and micropipettes. Besides, the procedure was carried out in laminar flow to prevent contamination. Two 96-well plates were used for a total of ten *N*-acylhydrazones and one positive control for each bacterium. The first plate included a positive control and four compounds while the second plate consisted of the remaining six compounds.

The columns of the 96 well plates were first assigned for the eleven compounds. 100 μL of the sterile MH broth was added to the four corners of each of the 96-well plate as the sterility control. Column 2 of the first plate acted as positive control and 50 μL of the 100 μg/mL streptomycin solution was added and diluted serially into each well of column 2 that contained 50 μL of MH broth. Then, 50 μL of bacteria suspension prepared in section **3.6.1.6** was added into each well to give the final concentration that ranged from 1.95 to 250 μg/mL. The above processes were repeated by replacing the streptomycin solution with *N*-acylhydrazones according to the table shown below. Solvent control was made at column 12 (row B-C) of each 96-well plate. 50 μL of sterile MH broth was added into the two wells, followed by the serial dilution of 50 μL of DMSO solution. Then, 50 μL of bacteria suspension was added to give the final concentration of 6.25 % and 12.5 %. Furthermore, column 12, row E was assigned for the growth control where 50 μL of bacteria suspension was added. After completing all the procedures, the 96-well plate was sealed with parafilm and incubated overnight at 37 ^{o}C.

Table 3.10: Arrangement of compounds in the two 96-well plate

First 96-well plate	**Compounds**	**Second 96-well plate**	**Compounds**
2	Streptomycin	3	*N*-acylhydrazones **SB 5** (4-Cl)
4	*N*-acylhydrazones **SB 9** (4-Me)	5	*N*-acylhydrazones **SB 4** (2-Cl)
6	*N*-acylhydrazones **SB 10** (4-NMe_2)	7	*N*-acylhydrazones **SB 6** (2,4-Cl_2)

8	*N*-acylhydrazones **SB 2** (2-OH)	9	*N*-acylhydrazones **SB 8** (4-F)
10	*N*-acylhydrazones **SB 3** (4-OH)	10	*N*-acylhydrazones **SB 7** (3,4-Cl_2)
-	-	11	*N*-acylhydrazones **SB 1** (H)

The next day, 20 µL of 0.4 µg/mL of INT solution prepared in section **3.6.1.5** was added into each well containing the mixture. The precaution step must be taken as INT dye is light-sensitive. Then, the 96-well plate was again incubated for 15 minutes at 37 ^{o}C (Eloff, 1998). The growth of the bacteria was observed by the colour change. The presence of reddish-pink colour implied the existence of bacterial activity. On the other hand, the colourless well indicated that the compounds at that concentration were able to inhibit bacterial activity. The MIC value where the lowest concentration of the compound that showed antibacterial activity was determined and recorded (Mogana, et al., 2020). Duplicate assays were done to obtain consistent and accurate results.

3.7 Calculation

1. Determination of mass of materials that needed in the synthesis.

Mass (g) = Number of moles (mol) x Molecular weight (g mol^{-1})

2. Determination of volume of materials that needed in the synthesis.

$$\text{Volume of reagent needed, mL} = \frac{\text{Mass of reagent used (mol)}}{\text{Molecular weight (g mol}-1)}$$

3. Determination of the percentage yield for the synthesised products.

$$\text{Percentage yield (\%)} = \frac{\text{Experimental mass of product (g)}}{\text{Theoretical mass of product (g)}} \times 100\%$$

4. Determination of the retardation factor, R_f value

$$R_f = \frac{\text{Distance travelled by sample from the baseline (cm)}}{\text{Distance travelled by solvent from the baseline (cm)}}$$

5. Conversion of $\frac{\mu g}{mL}$ to mM ($\frac{\mu mol}{mL}$)

$$\text{mM} = \frac{\frac{\mu g}{mL}}{\text{Molecular weight}} \text{ x } 1000$$

CHAPTER 4

RESULTS AND DISCUSSION

4.1 Synthesis of ester

4.1.1 Proposed mechanism for the synthesis of ester

Ester was produced which involved the condensation between hydrochloride and in the presence of Bronsted-acid (acetic acid). The nitrogen atom of the hydrochloride had lone pair electrons. Thus, it acted as a nucleophile to attack the carbonyl carbon of the ester that had a partial positive charge. As a result, hydrazone was formed when one water molecule was released as a by-product. When hydrazone was heated under acidic conditions, the tautomerization process occurred and it was converted to enehydrazine. Then, enehydrazine would experience rearrangement followed by a further tautomerization process that induced the formation of a ring. Finally, the desired ester was produced upon imine exchange and with the elimination of molecule as a by-product (Govaerts, et al., 2022).

4.2 Synthesis of carboxylic acid hydrazide

4.2.1. Proposed mechanism for the synthesis of carboxylic acid hydrazide

The carboxylic acid hydrazide was synthesised through the nucleophilic acyl substitution reaction at 80 ^{o}C. The reactants were ester produced in **Section 4.1** and hydrazine hydrate dissolved in absolute ethanol. The nucleophilic acyl substitution reaction started when the lone pair electrons of the nitrogen of hydrazine hydrate attacked the carbonyl carbon of the ester. As a result, a tetrahedral intermediate with an ethoxide ion was generated. With the expulsion of the ethoxide ion, a carbonyl group was formed. Then, a proton was immediately transferred to the ethoxide ion and carboxylic acid hydrazide was produced. Besides, ethanol was formed as the by-product (Mirfazli, et al., 2014).

4.2.2 Structure elucidation of carboxylic acid hydrazide

Carboxylic acid hydrazide is the key precursor for the desired product of this project which is *N*-acylhydrazone. The precursor was observed to be a light brown solid with a melting point range of 197 to 199 ^{o}C. The percentage yield of this precursor was calculated to be 46 %. The purity of the product was confirmed by using TLC analysis with the solvent system of hexane: ethyl acetate in the ratio of 1:1. The R_f value of this spot was determined to be 0.16.

Besides that, this precursor was also characterised with various spectroscopic methods likewise FT-IR, ^{1}H NMR, ^{13}C NMR, DEPT, HMQC as well as HMBC.

Physical Appearance	Light brown solid
Percentage yield (%)	46
Melting point (°C)	197-199
R_f value (*n*-Hexane: Ethyl acetate = 1:1)	0.16

Table 4.1: Summary of the physical properties of carboxylic acid hydrazide

Besides, carboxylic acid hydrazide was analysed by using FT-IR. Based on the IR spectrum with frequency ranging from 4000 to 400 cm^{-1} (**Figure 4.4**), it was observed that the N-H stretch in the carboxylic acid hydrazide was represented by the four sharp absorption bands at 3311 cm^{-1}, 3211 cm^{-1}, 3266 cm^{-1} and 3154 cm^{-1}. The four absorption bands included one proton from indole-NH, one proton from CO-NH and two signals from the symmetric and asymmetric NH_2 stretching. Furthermore, a strong absorption band that belonged to the aromatic C-H group was observed at 3043 cm^{-1}. Besides that, another medium and sharp peak found at 2950 cm^{-1} indicated the presence of the sp^3 C-H group. The presence of an amide carbonyl (C=O) functional group in the structure could be confirmed by the existence of a strong intensity and sharp absorption peak at 1655 cm^{-1}. Additionally, the stretching of the aromatic C=C functional group was found at 1579 cm^{-1}. It is a medium-

intensity and sharp vibrational band. There were a few significant peaks found at the lower field of the IR spectrum. For instance, a peak at 1045 cm^{-1} that represented the C-N functional group (Khan, et al., 2020). The spectral data of FT-IR for carboxylic acid hydrazide is summarized in **Table 4.2**.

Table 4.2: Summary of FT-IR spectral data of 2-(5-bromo-2-methyl-1*H*-indol-3-yl) acetohydrazide

Functional Group	**Wavenumber (cm^{-1})**
N-H/NH_2 stretch	3311, 3211, 3166, 3154
Aromatic C-H stretch (sp^2)	3043
sp^3 C-H stretch	2912
C=O stretch	1655
Aromatic C=C stretch (sp^2)	1579
C-N stretch	1045

The ^{1}H NMR spectra of carboxylic acid hydrazide are shown in **Figures 4.5** and **4.6**. It was found that the proton of NH (1-NH) was found at the highest chemical shift of δ 11.96. The proton of NH was deshielded by the conjugated ring system. Besides, the proton of the amide group (CO-NH) was determined to be a singlet peak at δ 10.12 due to the presence of both carbonyl and nitrogen groups. Furthermore, the proton of the NH_2 group showed a 2H and broad singlet signal at δ 4.44. These signals contributed by the NH, amide NH and NH_2 group all disappeared upon the addition of D_2O as shown in **Figure 4.7**. The deuterium had replaced the hydrogen of these groups. Thus, they were not detected by NMR. The situation was not observed when DMSO-d_6 was used as the solvent because DMSO-d_6 does not contain hydrogen that can be easily replaced (Manzano, 2018).

Apart from that, the aromatic protons of the benzene ring or more specifically H_6 was observed at δ 7.13 (dd, J = 8.6, 1.8 Hz). H_6 appeared as a doublet of doublets as it managed to couple with the neighbouring H_7 (δ 7.24, d, J = 8.6 Hz) and also form *W* coupling with the H_4 (δ 7.55, d, J = 1.8 Hz). Furthermore, the signals due to the methylene (H_8) and methyl (2-CH_3) protons were found as singlets at δ 3.42 and δ 2.51, respectively. The aliphatic proton will normally find at the lower chemical shift (Khan, et al., 2020).

The ^{13}C NMR spectrum of carboxylic acid hydrazide is shown in **Figure 4.8**. There was a total of eleven separate carbon resonances appeared in the ^{13}C

NMR spectrum. Two of them (C_8 and 2-CH_3) appeared in the upfield region while the other nine signals were found at the downfield region. The carbon signals were further distinguished by using DEPT experiments which included DEPT 45˚, DEPT 90˚ as well as DEPT 135˚ (**Appendix A2**). DEPT 135˚ helped to determine the methylene carbon as it appeared as negative peak. Besides, the three methine carbons were confirmed by DEPT 90˚.

The most deshielded carbon signal was determined to be at δ 170.5 and this belonged to the carbonyl carbon of the amide group. This situation happened because it is an sp^2 hybridized atom. Besides that, the oxygen and nitrogen atoms are more electronegative than the carbon atom. Thus, the oxygen and nitrogen species attracted electron density towards themselves, deshielding the carbon atom to a greater extent. Apart from that, the carbon signals between δ 115.3 to δ 145.4 were contributed by the eight aromatic carbons of the indole ring. On the other hand, the indole methylene (2-CH_3) and methyl carbon (C_8) provided signals at lower chemical shifts of δ 29.9 and δ 11.9, respectively.

In addition, heteronuclear multiple quantum coherence, HMQC and heteronuclear multiple bond correlation, HMBC which are grouped under 2D-NMR were used to elucidate the structure of carboxylic acid hydrazide. HMQC showed the direct one-bond coupling between the corresponding hydrogen and carbon. Thus, it was used to further confirm the chemical shift of the carbon atom. Based on the HMQC spectrum in **Appendix A3**, there was a total of five cross peaks found between δ_H 7.55/δ_C 130.7, δ_H 7.24/δ_C 122.7, δ_H

7.13/δ_C 132.8, δ_H 3.32/δ_C 29.9 and δ_H 2.41/δ_C 11.9. The hydrogen atoms from NH_2 and N-H did not show any HMQC correlation as they were not connected to carbon atoms.

Moreover, HMBC showed the long-range coupling between the proton and carbon over two to three bonds distance. In some circumstances, a four-bond distance is also allowed, especially in the aromatic ring system. The direct coupling between carbon and hydrogen was prohibited in HMBC. With the help of both HMQC and HMBC spectra, the quaternary carbon that is present in the structure of the carboxylic acid hydrazide could be figured out.

Based on the HMBC spectrum (**Appendix A4**), the methylene proton (H_8) at δ 3.32 showed four cross peaks. This meant that the H_8 could couple with four different carbons through two to three bonds. For example, H_8 showed a two-bond correlation with C_3, creating the first cross peak shown in the HMBC spectrum. Besides that, H_8 also showed three bond coupling with C_2 as well as C_{3a}. H_8 is three bonds distance away from the carbonyl carbon of the amide group. Hence, a cross peak was also observed. H_8 did not show a correlation with C_8 as this is a direct one-bond coupling. The NH proton from the amide group correlates with the carbonyl carbon through two-bond coupling.

Table 4.3: Summary of ^{1}H NMR (400 MHz) and ^{13}C NMR (100 MHz) spectral data of carboxylic acid hydrazide.

4.3 Synthesis of *N*-acylhydrazones SB 1- SB 10

4.3.1 Proposed mechanism for the synthesis of *N*-acylhydrazones SB 1- SB 10

The *N*-acylhydrazones **SB 1 – SB 10** were successfully synthesised by reacting the key precursor carboxylic acid hydrazide with a series of aromatic benzaldehydes via an acid-catalyzed condensation reaction. Firstly, the amino group of the carboxylic acid hydrazide that has lone pair electrons would act as a nucleophile to attack the carbonyl carbon of the benzaldehyde. As a result, an alkoxide ion was formed as the intermediate which would then be converted into carbinolamine once the proton was transferred from the nitrogen to oxygen atom. After that, the oxygen atom of the carbinolamine would accept a proton from the acid (catalyst). Hence, the hydroxyl group became a water molecule which functioned as a stable leaving group. Finally, *N*-acylhydrazones were produced with a loss of a proton from the nitrogen atom back to the catalyst. acid reformed at the end of the reaction and hence it is a catalyst. The mechanism of this reaction is shown in **Figure 4.9**.

4.3.2 Synthesis and characterisation of *N*-acylhydrazones SB 1- SB 10

A total of ten *N*-acylhydrazones **SB 1- SB 10** were successfully obtained by the reaction between carboxylic acid hydrazide and a series of substituted benzaldehydes. The catalyst used in this condensation reaction was acid which would be regenerated back at the end of the reaction. *N*-acylhydrazones **SB 1 – SB 10** were obtained in the range of 35 to 74 %. It was observed that the *N*-acylhydrazone with electron-donating group substituted on the phenyl ring would have higher yields as compared to others. For example, **SB 2** (2-OH) was obtained with good yield of 74 %. On the other hand, when the unsubstituted benzaldehyde (**SB 1**) was used, the percentage yield obtained was very low (35 %).

The products synthesised were observed to be light brown, brown or dark brown colour solid. Besides that, the melting point of the compounds produced ranged from 201 to 245 ^{o}C. TLC analysis was used to confirm the purity of each of the compounds generated. The solvent system utilised was a mixture of *n*-hexane: ethyl acetate in a 1:1 ratio. A single spot was observed for each compound and R_f values ranging from 0.39 to 0.63 were obtained. All the R_f values obtained were different from that of the precursor. This implied that the precursor completely reacted in the condensation reaction to form products. Furthermore, from the results obtained, it was found that **SB 4** (with 2-Cl substituted on the phenyl ring) had the greatest R_f value and travelled the longest distance. Hence it had the lowest polarity. It had a high affinity with

the non-polar mobile phase. On the other hand, **SB 3** (with 4-OH substituted on the phenyl ring) was observed to have the highest polarity because it travelled the least in the TLC system. It had stronger interaction with the polar stationary phase.

The summaries of the physical properties of *N*-acylhydrazones **SB 1- SB 10** are tabulated in **Table 4.4**. All the newly synthesised *N*-acylhydrazones were characterised with various spectroscopic methods likewise FT-IR, ^{1}H NMR, ^{13}C NMR, DEPT, NOE, 2D-HMQC and HMBC. *N*-acylhydrazones **SB 9** (4-CH_3 substituted) had been chosen as the representative compound for further structure elucidation.

SB	R_1	R_2	R_3
1	H	H	H

2	OH	H	H
3	H	H	OH
4	Cl	H	H
5	H	H	Cl
6	Cl	H	Cl
7	H	Cl	Cl
8	H	H	F
9	H	H	CH_3
10	H	H	$N(CH_3)_2$

Table 4.4: Summary of the physical properties of *N*-acylhydrazones SB 1- SB 10

Compound	Physical Appearance	Percentage yield (%)	R_f value (*n*-hexane: ethyl acetate = 1:1)
SB 1 (H)	Dark brown solid	35	0.50
SB 2 (2-OH)	Dark brown solid	74	0.53
SB 3 (4-OH)	Dark brown solid	52	0.39
SB 4 (2-Cl)	Light brown solid	67	0.63
SB 5 (4-Cl)	Brown solid	43	0.54
SB 6 (2,4-Cl_2)	Light brown solid	72	0.63
SB 7 (3,4-Cl_2)	Dark brown solid	42	0.53
SB 8 (4-F)	Light brown solid	57	0.56
SB 9 (4-Me)	Light brown solid	65	0.59
SB 10 (4-$NMe)_2$	Dark brown solid	41	0.49

4.3.3 FT-IR characterisation of *N*-acylhydrazones SB 1- SB 10

The FT-IR spectra of all the ten newly synthesised *N*-acylhydrazones were obtained and shown in **Figure 4.12** and **Appendices B1-B9**. By referring to the IR spectrum of *N*-acylhydrazones **SB 9** (4-CH_3 substituted), it was found that the strong N-H absorption bands were found at 3317 cm^{-1}, 3196 cm^{-1} and 3102 cm^{-1} (Mirfazli, et al., 2014). There were two N-H bonds present in the chemical structure as shown in **Figure 4.11**. The third N-H absorption peak might be due to the *cis/trans* rotamers that are present in the compound. Furthermore, the aromatic CH_3 stretching was found at 3056 cm^{-1}. It was a sharp and strong vibrational peak. Besides that, the strong and sharp absorption peak at 2910 cm^{-1} indicated the presence of sp^3 C-H stretch in the compound. The strong vibrational peak found at 1659 cm^{-1} implied that the C=O functional group present in the compound belonged to the secondary amide group. The presence of conjugation reduced the C=O signal to a lower wavenumber. Moreover, the aromatic C=C, C-N peaks were found at 1606 cm^{-1}, 1047 cm^{-1} respectively. All the absorption peaks were sharp. Apart from that, there is one significant peak that is able to distinguish the product from the precursor, which is the C=N signal. This situation happened because C=N functional group was absent in the precursor. For compound **SB 9**, the C=N absorption band was found to be a medium-intensity and sharp band at 1564 cm^{-1} (Oliveira, et al., 2022). In addition, the presence of an absorption peak at 814 cm^{-1} implied the existence of para-substituted compounds on the phenyl ring. This peak further confirmed the chemical structure of compound **SB 9**.

The FT-IR spectral data of *N*-acylhydrazones **SB 1 – SB 10** are summarized in **Table 4.5**.

Table 4.5: Summary of FT-IR spectral data for *N*-acylhydrazones **SB 1- SB 10**

Compound	**Wavenumber (cm^{-1})**											
	N-H	**Aromatic C-H**	**sp^3 C-H**	**C=O**	**C=N**	**Aromatic C=C**	**C-N**		**C-Cl**	**C-F**	**O-H**	**Ortho/Para Disubstituted**
SB 1 (H)	3310, 3192	3050	2902	1679	1601	1556	1046		-	-	-	-
SB 2 (2-OH)	3357, 3228	3037	2909	1667	1615	1577	1047		-	-	*	753 (o)
SB 3 (4-OH)	3346, 3278	3163	2977	1648	1610	1586	1045		-	-	*	808 (p)
SB 4 (2-Cl)	3421, 3298, 3237	3058	2905	1671	1594	1577	1047		795	-	-	754 (o)

SB 5 (4-Cl)	3398, 3311, 3185	3066	2951	1657	1603	1578	1047		789	-	-	817 (p)
SB 6 (2,4-Cl_2)	3383, 3234, 3191	3083	2905	1669	1596	1551	1048		800, 819	-	-	-
SB 7 (3,4-Cl_2)	3407, 3289, 3179	3089	2951	1666	1600	1552	1047		792, 819	-	-	-
SB 8 (4-F)	3412, 3303, 3196	3050	2914	1677	1604	1560	1047		-	1072	-	831 (p)
SB 9 (4-Me)	3417, 3296, 3202	3056	2910	1659	1606	1564	1047		-	-	-	814 (p)
SB 10 (4-$NMe)_2$	3410, 3287, 3182	3027	2891	1668	1612	1524	1067		-	-	-	822 (p)

* OH peaks were overlapping with the NH_2 peaks, so it is unable to determine the OH peak values.

4.3.4 NMR structural characterisation of *N*-acylhydrazones SB 4, SB 5, SB 6, SB 8, SB 9

4.3.4.1 ^{1}H NMR structural characterisation of *N*-acylhydrazones SB 4, SB 5, SB 6, SB 8, SB 9

Some of the newly synthesised compounds (*N*-acylhydrazones **SB 4**, **SB 5**, **SB 6, SB 8, SB 9**) were analysed by using 1D-NMR (^{1}H NMR, ^{13}C NMR, DEPT) as well as 2D-NMR (HMQC, HMBC). DMSO-d_6 was used as the solvent. The other compounds were not characterised by NMR due to the breakdown of NMR spectrometer.

The formation of the *N*-acylhydrazones **SB 4, SB 5, SB 6, SB 8** and **SB 9** was confirmed by the ^{1}H NMR spectral data (**Figures 4.13, 4.14** and **Appendices C1-C4**). Besides, the absence of the amino NH_2 peak at δ 4.14 in this spectrum implied that the condensation reaction occurred completely and the precursor was fully transformed into the desired product. The compounds would mostly exist in (*E*)-configuration due to the steric hindrance around the imine bond. In addition, the presence of extra peaks as compared to the precursor indicated the formation of the product.

N-acylhydrazones in the DMSO-d_6 solution can exist as *cis*/*trans* amide conformers due to rotation of the amide CONH single bond as shown in **Figure 4.13**. By referring to the compound **SB 9** (4-CH_3 substituted), it was found that the two sets of 1H singlet signal at δ 11.35 - 11.40 and δ 7.63 - 7.17

which represented the essential functional groups in *N*-acylhydrazone which are the amide and imine group respectively. Moreover, the proton from indole-NH was found downfield (δ 11.98 - 10.06). These protons' signals appeared as duplicates due to the existence of *cis* and *trans* rotamers. The inversion of the amide bond led to the formation of these stereoisomers. NMR is suitable and capable to distinguish the *cis* and *trans* conformers presence in the compound.

According to the literature, the amide proton of the compound with *trans* conformers would appear at the higher chemical shift while that one with *cis* conformers was found at a more shielded region. Besides, *cis* isomers appeared in a greater percentage. By applying PM7 method, it was proven that *cis* rotamer was predominant in the *N*-acylhydrazone compound synthesised. This situation happened because the *cis* isomers are more stable in the DMSO-d_6 solvent (Kumar et al., 2017). Hence, in compound **SB 9**, the signal at δ 11.30 with lower intensity was assigned to be the peak for the amide proton of the *trans* rotamer. Besides, the peak at δ 11.25 was contributed by the amide proton of *cis* rotamer of compound **SB 9**. The singlet peak observed at δ 11.98 with higher intensity belonged to the signal from the proton of *cis* rotamer. On the other hand, the NH of the *trans* isomer had a weaker signal at δ 11.03. In addition, the imine proton with higher intensity at δ 7.93 was assigned to be *cis* configuration since *cis* isomer is predominant. The lower intensity peak at the downfield region (δ 8.17) was the peak of the imine proton of the *trans*

isomer. According to the research done by Bennia and his group, it was concluded that *cis* proton will normally be more shielded than that of the *trans* proton, which matched with the result obtained for compound **SB 9** (Bennia, et al., 2018). The ^{1}H NMR spectral data of *N*-acylhydrazone derivatives **SB 4, SB 5, SB 6, SB 8** and **SB 9** are summarized in **Table 4.6**.

4.3.4.2 ^{13}C NMR, DEPT and 2D-NMR structural characterisation of *N*-acylhydrazones SB 4, SB 5, SB 6, SB 8, SB 9

The formation of the *N*-acylhydrazone derivatives was confirmed by the ^{13}C NMR spectra. The ^{13}C NMR spectra of compounds **SB 9** and **SB 4, SB 5, SB 6** and **SB 8** are shown in **Figure 4.16**, **Figure 4.17** and **Appendices E1-E4** respectively. It was observed that the signal of imine carbon (N=CH) was found at δ 128.4 to δ 136.9. This is an extra signal that does not shown in carboxylic acid hydrazide. Besides, carbonyl amide of CO-NH was detected at the higher chemical shift (δ 157.5 to δ 175.2).

Compound **SB 9** was chosen as the representative compound for further structure elucidation and discussion. The presence of extra peaks as compared to the precursor indicated the formation of the product. In addition, the ^{13}C NMR spectrum of this compound also indicated the duplication of signals for almost all of the carbons due to the existence of *cis* and *trans* rotamers. The carbonyl carbon signal with a higher chemical shift (δ 174.9) belonged to the *cis* stereoisomer. Besides, the carbon resonance with lower intensity at δ 163.5 was assigned to the *trans* conformer. Furthermore, the signals of *cis* and *trans* imine carbon (N=CH) were observed at δ 136.9 and δ 148.6, respectively (Oliveira, et al., 2022). Additionally, the aromatic carbon signals that arose from the phenyl ring were found in the region of δ 114.7 to δ 145.2. The two carbon resonances observed in the lower chemical shift of δ 30.7 (*trans*) and δ 28.4 (*cis*) implied the presence of the methylene carbon, C_8 that attached to the amide group. Besides that, the methyl (2-CH_3) was indicated by another pair

of carbon resonances that were found at δ 12.1 (*cis*) and δ 12.0 (*trans*). The ^{13}C NMR spectral data of compounds **SB 4, SB 5, SB 6, SB 8** and **SB 9** are summarised in **Table 4.7**.

Besides that, DEPT, HMQC and HMBC were used to provide more information to elucidate the structure of the newly synthesised compounds. By referring to the DEPT 135˚ spectrum shown in **Figure 4.18**, it was further confirmed that the signals at δ 30.7 and δ 28.4 belonged to the methylene carbon (C_8) as these two peaks showed negative signals in the spectrum. Furthermore, the positive peaks of methine carbons (CH) were determined by using DEPT 90˚. For instance, imine carbon (N=CH), C3'/, C2'/6', C6, C4 and also C7 were detected. Moreover, the methyl carbon (CH_3) at 2-CH_3 (δ 12.1 and δ 12.0) as well as 4'-CH_3 (δ 21.5) were determined successfully. The remaining carbons that not mentioned above belonged to the quaternary carbon (C2, C3, C3a, C5, C7a, C1' and C4').

Apart from that, the HMQC spectrum of compound **SB 9** (4-CH_3 substituted) is shown in **Figure 4.19**. HMQC showed the one bond (direct) correlation between the hydrogen and its corresponding carbon. It was found that the *cis* (δ 8.18) and *trans* (δ 7.94) signals of imine proton coupled with their corresponding *cis* (δ 136.9) and *trans* (δ 133.6) imine carbon. Thus, by using HMQC, the *cis* and *trans* signals of the imine carbon could be differentiated correctly. Additionally, HMBC managed to detect the two or three-bond coupling between the carbon and its neighbouring hydrogen. The direct bond

correlation was forbidden in HMBC. The HMBC spectrum of compound **SB 9** (4-CH_3 substituted) is shown in **Figure 4.20**. This spectrum showed the correlation between the *trans* amide proton (two bonds distance) with the *trans* imine carbon (three bonds distance) as well as the *trans* carbonyl carbon of the amide group. Besides that, the H-8 showed two bonds coupling with C-3 and the amide carbon as well as three bonds coupling with C-3a and C-2. The correlations between the imine proton with C-2'/C-6' and also C-3'/C-5' implied that the imine group was attached to a phenyl ring and thus indicated the presence of the product. In short, with the help of DEPT, HMQC and also HMBC, the quaternary carbons and the connection between the molecules could be determined.

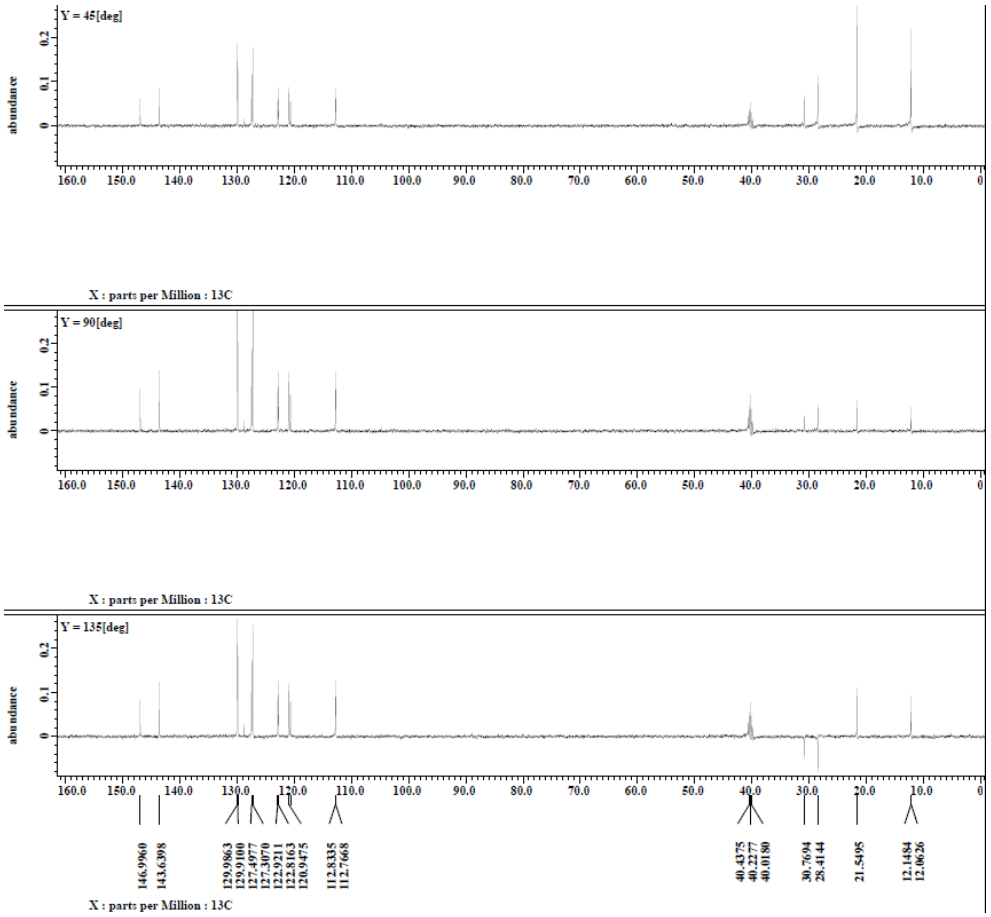

Figure 4.18: DEPT spectrum of *N*-acylhydrazone **SB 9** (4-CH_3 substituted)

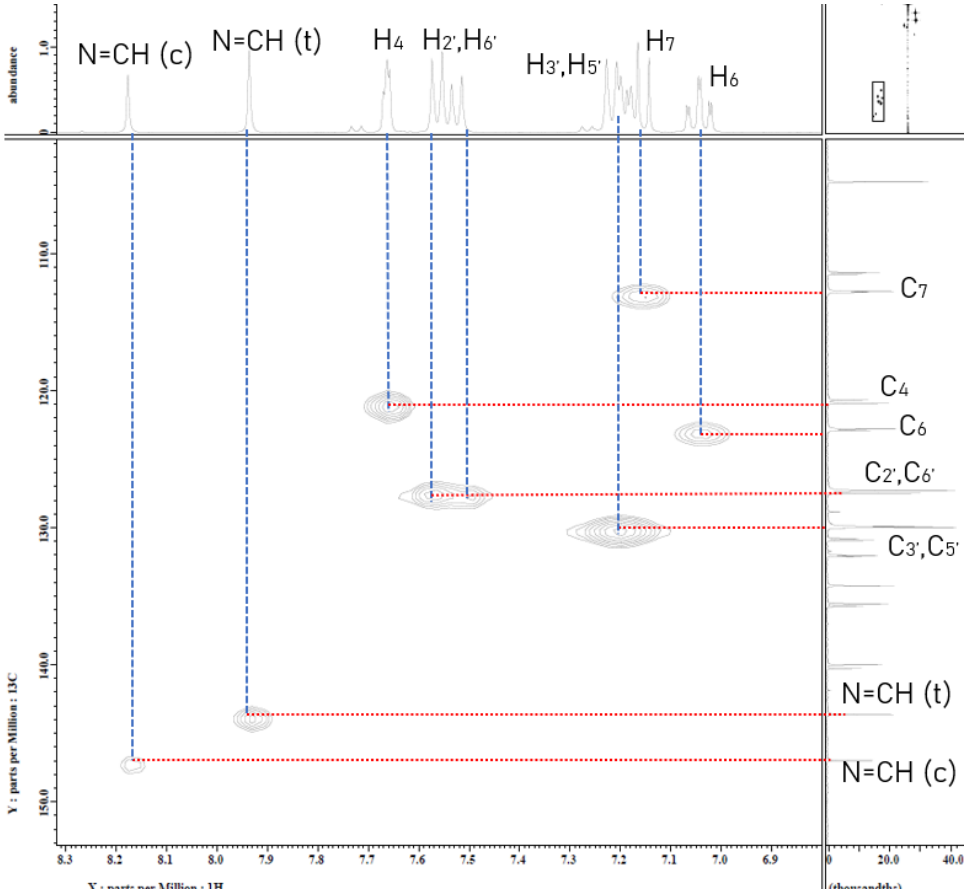

Figure 4.19: HMQC spectrum of *N*-acylhydrazone **SB 9** (4-CH_3 substituted)

4.3.5 Conformational study of *N*-acylhydrazones SB 4, SB 5, SB 6, SB 8, SB 9

4.3.5.1 Determination of the relative configuration of the imine double bond and the conformation of CO-NH bond

The newly synthesised *N*-acylhydrazones can exist as (*E*) or (*Z*) geometrical isomers in DMSO-*d*6 solution due to rotation along C=N–NH bond as shown in **Figure 4.21**. Hence, Differential Nuclear Overhauser Effect (NOE) experiments which managed to provide information such as the spatial arrangement of atoms were done on the compounds (**SB 5, SB 6, SB 8, SB 9**). The remaining product was unable to characterise by using NOE experiments due to the instrument breaking down. The NOE spectra of compound **SB 9** were shown in **Figure 4.23** and **Figure 4.24** while that for the other compounds were shown in **Appendices G1-G6**. Compound **SB 9** was chosen as the representative compound for the discussion.

Based on the NOE spectra of compound **SB 9**, it was found that the irradiation of the amide (CO-NH) proton resulted in the NOE enhancement (10 %) of the imine proton (N=CH). The nuclear spins of the amide proton and imine proton had interaction with each other. This interaction caused a shift of nuclear spin polarisation from amide proton to imine proton. Thus, the NMR signal of the imine proton was elevated by 10 % whereas the signal of the amide proton was suppressed. Furthermore, irradiation of the imine (N=CH) proton at (*cis*) also showed the NOE enhancement (11 %) of the amide (CO-NH) proton at (*cis*). A similar trend was also observed for compounds **SB 5**, **SB 6** as well as **SB 8**. This experiment concluded that the distance between the amide and imine groups was close. Hence, this supported the statement that *N*-acylhydrazone will always exist in (*E*)- and *cis* configuration (Xie, et al., 2020). This situation happened because it is too far for the amide and imine proton to react if the compound existed in (*Z*)- as well as *trans* configuration. The different configurations of compound **SB 9** were shown in **Figure 4.22**. In addition, the percentage of stereoisomers of *N*-acylhydrazones **SB 5, SB 6**, **SB 8**, and **SB 9** in DMSO-d_6 are tabulated in **Table 4.8**.

Apart from that, the ratios of the *cis/trans* amide stereoisomers were determined from the integration areas of the amide (CO-NH) signal in the ^{1}H NMR spectra of the compound synthesised and were tabulated in **Table 4.9**. The integration area of the proton spectra of *N*-acylhydrazones are shown in **Figure 4.25** (**SB 9**) and also **Appendices H1-H4** (**SB 4, SB 5, SB 6, SB 8**).

The results implied that the percentage of *cis* and *trans* rotamers of *N*-acylhydrazones were found in the range of 60 % - 63 % and also 37 % - 40% respectively. It was concluded that the newly synthesised *N*-acylhydrazones were preferred to exist in *cis* isomer about the amide bond. Furthermore, the higher peak intensity of *cis* conformers (as shown in the ^{1}H and ^{13}C NMR spectra) also supports this statement.

Table 4.8: Summary of percentage of isomers of *N*-acylhydrazone compounds in DMSO-d_6

Compound		**SB 5**	**SB 6**	**SB 8**	**SB 9**
Isomer (%)	*E*	100	100	100	100
	Z	0	0	0	0

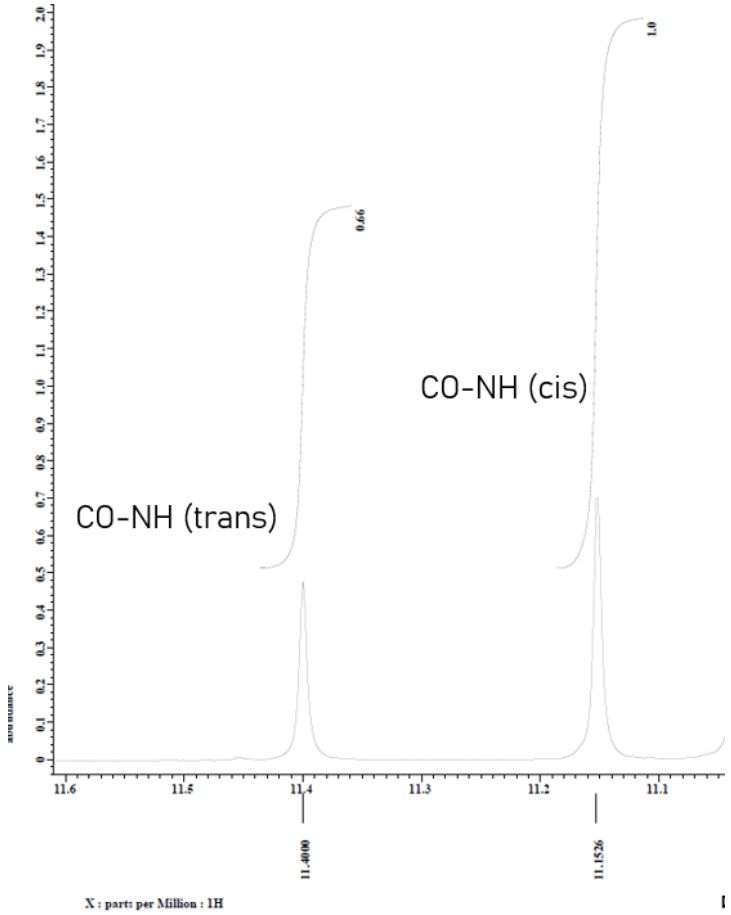

Figure 4.25: The integration area of CO-NH proton of *N*-acylhydrazone **SB 9** (4-CH_3 substituted)

4.3.5.2 Rotational barriers around the CO-NH bond of *N*-acylhydrazones SB 5, SB 6, SB 8 and SB 9

Dynamic NMR experiments were carried out to determine the energy barriers of the rotation of *cis/trans* conformers for the newly synthesised *N*-acylhydrazones. Besides, the rate constant of the *cis/trans* equilibrium had also been investigated. The rate constant of the *cis/trans* equilibrium, k_c can be calculated by referring to the Gutowsky equation where $k_c = \frac{\pi \Delta v}{\sqrt{2}}$. Δv represented the peak separation of the two singlet peaks of the amide bond in Hertz. The two singlet peaks are the signal from the *cis* and *trans* rotamers of the *N*-acylhydrazone. The energy of the rotational barrier or Gibb's free energy of the activation, $\Delta G^{\neq}$ can then be figured out by using the Eyring equation where $\Delta G^{\neq}$ = 19.14 T_c (10.32 + $\log \frac{T_c}{k_c}$)$\times 10^{-3}$. The unit of $\Delta G^{\neq}$ is kJ mol^{-1}. The T_c, in Kelvin, is the coalescence temperature when the two separate singlet peaks merged to become a single peak. At T_c, the *cis* and *trans* signals coalesce due to the high exchange rate. Thus, the difference in the chemical shift of these two conformers is small until NMR is unable to distinguish them (Aarjane, Slassi and Amine, 2020).

In this study, the Dynamic NMR experiments were performed in DMSO-d_6 for compounds **SB 5**, **SB 6**, **SB 8** and **SB 9**. This was carried out by increasing the temperature of ^{1}H NMR analysis from 296.15 to 373.15 K. At 373.15 K, the *cis* and *trans* signals were observed as a single averaged peak for all the *N*-acylhydrazones mentioned. The Dynamic NMR spectra of compound **SB 9** is

shown in **Figure 4.27** and the one for **SB 5**, **SB 6** and **SB 8** are shown in **Appendices I1-I3**. Compound **SB 9** (4-CH_3 substituted) was again chosen for the discussion.

Furthermore, the results for restricted rotation about the amide bond for the other three compounds are tabulated in **Table 4.10**. It was concluded that the coalescence temperatures of the newly synthesised *N*-acylhydrazones were observed in the range of 353.15 to 363.15 K. Besides that, the energies of the rotational barrier were calculated to be between 82.16 kJ mol^{-1}. These quantities of energy were required to rotate the molecule around the amide (CO-NH) bond.

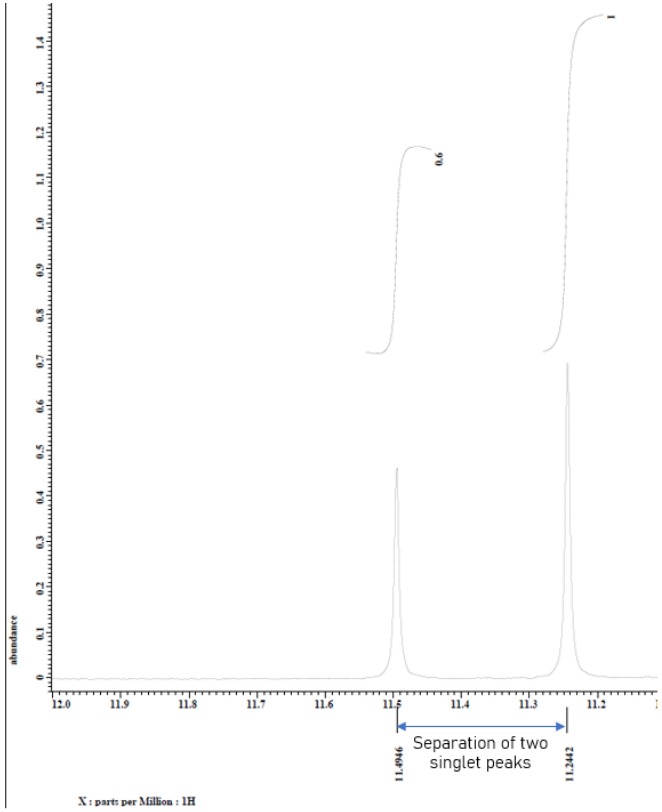

Figure 4.26: Separation of the two singlet peaks of amide bond for *N*-acylhydrazone **SB 9** (4-CH_3 substituted)

4.4 Antibacterial activity of *N*-acylhydrazones SB 1- SB 10

4.4.1 Determination of minimum inhibitory concentration (MIC) value

All the *N*-acylhydrazones **SB 1- SB 10** synthesised were evaluated for their *in vitro* antibacterial activity against two Gram-positive bacteria and one Gram-negative bacteria by using the broth microdilution method. The two Gram-positive bacteria included *Bacillus subtilis* (ATCC 6633) and *Staphylococcus aureus* (ATCC 6538), whereas the Gram-negative bacteria evaluated was *Pseudomonas aeruginosa* (ATCC 27853). The lowest concentration of the newly synthesised compound with the absence of bacterial growth (well that did not turn red) was observed and recorded as the minimum inhibitory concentration (MIC) value. The iodonitrotetrazolium chloride (INT) dye would be reduced to the insoluble pinkish-red formazan dye in the existence of respiratory activity. The colour change induced by INT was permanent (Štumpf, et al., 2020). The lower MIC value implied that the compound showed more powerful antibacterial activity against that particular bacterial strain. The results of the antibacterial activity are tabulated in **Table 4.11**. Besides, the order of the antibacterial potential of the tested compounds against the three bacterial strains was arranged in **Table 4.12**. Besides, **Figure 4.26** to **Figure 4.28** showed the demonstration of the inhibition effect of the *N*-acylhdyrazones against three different types of bacteria. Streptomycin was used as the positive control in this assay as its MIC range activity is similar to that of the *N*-acylhdyrazones synthesised in this study.

Based on the MIC value shown, it was found that *N*-acylhydrazone **SB 7** (with 3,4-Cl_2 disubstituted on the phenyl ring) exhibited excellent antibacterial activity against both of the Gram-positive bacteria strains of *Bacillus subtilis* and *Staphylococcus aureus* with the MIC value of 31.25 μg/mL and 15.63 μg/mL, respectively. Apart from that, *N*-acylhydrazone **SB 1** (with H substituted) showed moderate antibacterial activity against *Bacillus subtilis* with the MIC value of 62.5 μg/mL. The other compounds did not exhibit antibacterial activity as their MIC values were high (250 μg/mL or 125 μg/mL). This result implied that the antibacterial activity is highly dependent on the substituents on the phenyl ring.

The significant antibacterial activity of the compound **SB 7** was attributed to the existence of the substituent in the 3' and 4' positions of the phenyl ring. According to the research done, substituent displayed promising antibacterial activity against Gram-positive bacterial strains, such as *Enterococcus faecalis, Staphylococcus aureus* and *Streptococcus pyogenes* (Serafim, et al., 2019). Besides, another group of researchers also demonstrated that substituted hydrazone had exhibited good antibacterial activity against the *Bacillus subtilis* strain (Singh, et al., 2019).

However, when one of the chloro groups shifted to 2' position, the compound lost its antibacterial activity, as shown in compound **SB 6** where its MIC value was 125 μg/mL. Furthermore, the results obtained also showed that compounds with mono chloro substituted (**SB 4** and **SB 5**) also exhibited poor

antibacterial activity (250 μg/mL, 125 μg/mL). This result indicated that only compound **SB 7** with that specific 3,4-dichloro groups on the phenyl ring managed to inhibit the visible growth of the two Gram-positive bacteria investigated in this study.

N-acylhydrazones **SB 2**, **SB 3**, **SB 9** and **SB 10** are grouped as electron-donating substituents while *N*-acylhydrazones **SB 4** to **SB 8** halogenated compounds consist of electron-withdrawing groups. The presence of an electron-withdrawing group is trusted to be able to enhance the antibacterial activity of *N*-acylhydrazone. The electron-withdrawing group reduce the electron density in the phenyl ring, thus enhancing the cationic behaviour of the compound. Thus, the compound **SB 7** has the greater capability to penetrate through the cell wall of bacteria and disrupt their metabolism. Furthermore, the presence of an electron-withdrawing group will cause the compound to be more acidic. When the acidity increased, the two Gram-positive bacteria could not withstand the acidic environment which led to cell death (Radhakrishnan, et al., 2016).

Unfortunately, the detailed mechanism of the *N*-acylhydrazone in killing bacteria is not completely investigated. Some researchers pointed out that *N*-acylhydrazone managed to produce reactive oxygen species (ROS), an unstable free radical that reacts with other molecules in the bacterial cells actively. Examples of ROS included hydrogen peroxide (H_2O_2), superoxide ($O_2^{\cdot -}$) as well as hydroxy radical ($^{\cdot}OH$). When a large amount of ROS

accumulated in the cell, the bacteria cell will experience oxidative stress (Pizzino, et al., 2017). Oxidative stress is a phenomenon where the production of ROS exceeds the removal of the species. Consequently, apoptosis which leads to cell death will be induced by the intracellular reactive oxygen species. As a result, the bacteria cells can be killed. According to the research done, it was found that the presence of an indole-based *N*-acylhydrazone compound increased the concentration of ROS in the cell (Sreenivasulu, et al., 2019).

Table 4.12: The order of antibacterial potential of *N*-acylhydrazones SB 1 – SB 10 against bacterial strains

Bacteria strains	**Order of antibacterial potential of *N*-acylhydrazones SB 1 – SB 10**
Bacillus subtilis (ATCC 6633)	**SB 7** > **SB 1** > **SB 2, SB 3, SB 5, SB 6, SB 9, SB 10** > **SB 4, SB 8**
Staphylococcus aureus (ATCC 6538)	**SB 7** > **SB 2, SB 4, SB 5, SB 6, SB 8, SB 9, SB 10** > **SB 1, SB 3**
Pseudomonas aeruginosa (ATCC 27853)	All compounds obtained the same MIC value.

CHAPTER 5

CONCLUSION

5.1 Conclusion

In this study, the key precursor for the synthesis of *N*-acylhdyrazones which is the carboxylic acid hydrazide was successfully synthesised with a percentage yield of 46 %. Besides, a total of ten *N*-acylhdyrazone and its derivatives were produced through the condensation reaction of carboxylic acid hydrazide with a series of substituted benzaldehydes. The percentage yield of the products generated was within the range of 35 to 74 %. Wherase, the melting point of the compounds was in the range of 201 to 245 ^{o}C.

Furthermore, the structure of the carboxylic acid hydrazide and *N*-acylhdyrazones synthesised were elucidated by using various spectroscopic methods such as FT-IR, 1D-NMR (^{1}H NMR, ^{13}C NMR, DEPT) and also 2D-NMR (HMQC, HMBC). NOE experiments were also done for a few compounds. The NOE experiments revealed that the products generated existed as (*E*)-geometry isomer. The *cis/trans* conformers of the compounds were figured out by using the integration area of the CO-NH proton in the ^{1}H NMR spectra. Moreover, the results from Dynamic NMR experiments indicated that the coalescence temperature, T_c for the CO-NH signals were observed in the range of 363.15 K. Gibb's free energy for activation of

compounds **SB 5**, **SB 6**, **SB 8** and **SB 9** were calculated to be 75.26 kJ mol^{-1}. These are the energies required to rotate the conformers around the amide bond.

Apart from that, the antibacterial activities of the synthesised *N*-acylhdyrazones were evaluated by using the broth microdilution method successfully. The bacteria investigated included two Gram-positive bacteria which are *Bacillus subtilis* and *Staphylococcus aureus* as well as one Gram-negative bacterium that was *Pseudomonas aeruginosa*. It was found that compound **SB 7** exhibited excellent antibacterial activity on both Gram-positive bacteria. The minimum concentrations of compound **SB 7** required to inhibit the visible growth of *Bacillus subtilis* and *Staphylococcus aureus* were recorded as 31.25 μg/mL and 15.63 μg/mL respectively. Furthermore, compound **SB 1** also showed moderate antibacterial activity on *Bacillus subtilis* with a MIC value of 62.5 μg/mL.

5.2 Future prospects

The newly synthesised compound can also be analysed by using mass spectrophotometer to figure out the mass-to-charge ratio (*m*/*z*) and thus determine the exact molecular weight of the compounds. Moreover, the compound synthesised can be characterised by using CHN analyser to determine the carbon, hydrogen as well as nitrogen elemental content. An extensive study on the synthesis of *N*-acylhydrazones with other benzaldehydes especially with an electron-withdrawing group substituted can be carried out to discover a more potent antibacterial agent. This can helps to overcome the multidrug-resistant bacteria problem. Apart from that, different biological activities such as antifungal, antioxidant and cytotoxicity can be further studied on the synthesised *N*-acylhydrazone and its derivatives.

REFERENCES

Aarjane, M., Slassi, S. and Amine, A., 2021. Novel series of *N*-acylhydrazone based on acridone: Synthesis, conformational and theoretical studies. *Journal of Molecular Structure*, 1225, pp. 1-9.

Balouiri, M., Sadiki, M. and Ibnsouda, S.K., 2016. Methods for in vitro evaluating antimicrobial activity: A review. *Journal of Pharmaceutical Analysis*, 6(2), pp. 71-79.

Bennia, S. et al., 2018. Density functional theory based study on structural, vibrational and NMR properties of *cis – trans* fulleropyrrolidine mono-adducts. *PLoS One*, 13(11), pp. 1-8.

Ceramella, J. et al., 2022. A review on the antimicrobial activity of Schiff bases: Data collection and recent studies. *Antibiotics*, 11(2), pp. 191-213.

Cirillo, P.F., Caccavale, A. and DeLuna, A., 2021. Greener Fischer indole synthesis using a steroidal ketone in a conductively heated sealed-vessel reactor for the advanced undergraduate laboratory. *Journal of Chemical Education*, 2021(98), pp. 567-571.

Clinical and Laboratory Standards Institute, 2017. Performance standards for antimicrobial susceptibility testing: Twentiy-first information supplement. CSLI Supplement M100-S21, 31(1), pp.165.

Coimbra, E.S. et al., 2019. Synthesis, biological activity, and mechanism of action of new 2-pyrimidinyl hydrazone and *N*-acylhydrazone derivatives, a potent and new classes of antileishmanial agents. *European Journal of Medicinal Chemistry*, 184, pp. 111742-111753.

Dadashpour, S. and Emami, S., 2018. Indole in the target-based design of anticancer agents: A versatile scaffold with diverse mechanisms. *European Journal of Medicinal Chemistry*, 150, pp. 9-29.

Eloff, J.N., 1998. A sensitive and quick microplate method to determine the minimal inhibitory concentration of plant extracts for bacteria. *Planta Medica*, 64(8), pp. 711-712.

Elewa, N.A., 2020. *Synthesis, NMR-studies and biological activities evaluation of new series of tris-acylhydrazones of citric acid*. MSc Thesis, Al-Azhar University-Gaza.

Filho, J.M.S. and Pinheiro, S.M., 2017. Stereoselective, solvent free, highly efficient synthesis of aldo- and keto-*n*-acylhydrazones applying grindstone chemistry. *Green Chemistry*, 19, pp. 2212-2224.

Govaerts, S. et al., 2022. A halogen-atom transfer (xat)-based approach to indole synthesis using aryl diazonium salts and alkyl iodides. *Organic Letters*, 24, pp. 7883-7887.

Haj, N.Q., Mohammed, M.O. and Mohammood, L.E., 2020. Synthesis and biological evaluation of three new chitosan Schiff base derivatives. *ACS Omega*, 5(23), pp. 13948-13954.

Heravi, M.M. et al., 2017. Fischer indole synthesis applied to the total synthesis of natural products. *RSC Advances*, 7, pp. 52852-52887.

Humphrey, G.R. and Kuethe, J.T., 2006. Practical methodologies for the synthesis of indoles. *Chemical Reviews*, 106, pp. 2875-2911.

Hussain, Z. et al., 2016. Metal complexes of Schiff's bases containing sulfonamides nucleus: A review. *Research Journal of Pharmaceutical, Biological and Chemical Sciences*, 7(5), pp. 1008-1025.

Jagadeesan, S. and Karpagam, S., 2023. Novel series of *N*-acyl substituted indole based piperazine, thiazole and tetrazoles as potential antibacterial, antifungal, antioxidant and cytotoxic agents, and their docking investigation as potential Mcl-1 inhibitors. *Journal of Molecular Science*, 1271, pp. 1-10.

Khan, M.S., Siddiqui, S.P. and Tarannum, N., 2017. A systematic review on the synthesis and biological activity of hydrazide derivatives. *Hygeia Journal for Drugs and Medicines*, 9(1), pp. 61-79.

Kumar, P. et al., 2017. Design, synthesis, conformational and molecular docking study of some novel acyl hydrazone based molecular hybrids as antimalarial and antimicrobial agents. *Chemistry Central Journal*, 11(115), pp. 1-14.

Malik, M.A. et al., 2018. Heterocyclic Schiff base transition metal complexes in antimicrobial and anticancer chemotherapy. *Medicinal Chemistry Communications*, 9(3), pp. 409-436.

Manzano, C. M., 2018. *Transition metal complexes with ibuprofen hydrazide; synthesis, characterization and biological assays*. MSc Thesis, Universidade Estadual de Campinas.

Mirfazli, S.S. et al., 2014. *N*-substituted indole carbohydrazide derivatives: synthesis and evaluation of their antiplatelet aggregation activity. *DARU Journal of Pharmaceutical Sciences*. 22(1), pp. 65-74.

Moeketse, T.N. et al., 2022. Microwave-assisted synthesis of Schiff base metal-ligand complexes with copper and nickel centres for electrochemical in vitro sensing of nitric oxide in an aqueous solution. *Chemosensors,* 10(5), pp. 175-196.

Mogana, R. et al., 2020. Antibacterial activities of the extracts, fractions and isolated compounds from *Canarium patentinervium* miq. against bacterial clinical isolates. *BMC Complementary Medicine and Therapies*, 20(55), pp. 1-11.

National Center for Biotechnology Information, 2022. *PubChem Compound Summary for CID 5447130, Nitrofurazone.* [online] Available at: < https://pubchem.ncbi.nlm.nih.gov/compound/Nitrofurazone> [Accessed 4 November 2022].

Oliveira, F.A. et al., 2022. Evaluation of antiplasmodial activity in silico and in vitro of *N*-acylhydrazone derivatives. *BMC Chemistry,* 16(50), pp. 1-13.

Pereira, T.M. et al., 2016. Microwave-assisted synthesis and photophysical studies of novel fluorescent *N*-acylhydrazone and semicarbazone-7-OH-coumarin dyes. *New Journal of Chemistry*, 40(10), pp. 8846-8854

Pizzino, G. et al., 2017. Oxidative stress: Harms and benefits for human health. *Oxidative Medicine and Cellular Longevity*, 2017, pp. 1-13.

Popiolek, L. and Biernasiuk, A., 2017. Synthesis and investigation of antimicrobial activities of nitrofurazone analogues containing hydrazide-hydrazone moiety. *Saudi Pharmaceutical Journal*, 25(7), pp. 1097-1102.

Radhakrishnan, K. et al., 2016. Synthesis and antimicrobial activity of 2-benzylidene-1,3-indandiones: A structure-reactivity study. *Der Chemica Sinica*, 7(4), pp. 1-7.

Rahaman, K.S.S. et al., 2021. A comprehensive knowledge on review of indole derivatives. *International Journal of Life science and Pharma Research*, 1(4), pp. 19-24.

Rasheed, E.Q.A. et al., 2014. Synthesis and study properties physical and biological of some dihydrazone derivatives. *Chemistry and Materials Research*, 6(10), pp. 17-24.

Rodrigues, D.A. et al., 2016. Design, synthesis, and pharmacological evaluation of novel *N*-acylhydrazone derivatives as potent histone deacetylase 6/8 dual inhibitors. *Journal of Medicinal Chemistry*, 59(2), pp. 655-670.

Shah, S.S. et al., 2020. Synthesis and antioxidant activities of Schiff bases and their complexes: An updated review. *Biointerface Research in Applied Chemistry*, 10(6), pp. 6936-6963.

Shamsabadi, A. and Chudasama, V., 2016. An overview of the synthesis of acyl hydrazides from aldehydes and reactions of products therof. *Organic & Biomolecule Chemistry*, 15, pp. 17-33.

Silva, M.F. et al., 2020. Design, synthesis and biological evaluation of novel triazole *n*-acylhydrazone hybrids for Alzheimer's disease. *Molecules*, 25(14), pp. 3165-3182.

Singh, P. et al., 2019. Synthesis of 2-(3,4-dichloro-benzoyl)-benzoic acid hydrazide derivatives and assessment of antimicrobial efficacy against *E. coli* and *B. subtilis*. *World Journal of Pharmaceutical Research*, 8(13), pp. 857-869.

Song, Z. et al., 2019. Base promoted synthesis of novel indole-dithiocarbamate compounds as potential anti-inflammatory therapeutic agents for treatment of acute lung injury. *European Journal of Medicinal Chemistry*, 171, pp. 54-65.

Sreenivasulu, R. et al., 2019. Synthesis, antiproliferative and apoptosis induction potential activities of novel bis(indolyl)hydrazide-hydrazone derivatives. *Bioorganic & Medicinal Chemistry*, 27(6), pp. 1043-1055.

Štumpf, S. et al., 2020. The effect of growth medium strength on minimum inhibitory concentrations of tannins and tannin extracts against *E. coli*. *Molecules*, 25(12), pp. 1-14.

Thota, S. et al., 2018. *N*-acylhydrazones as drugs. *Bioorganic & Medicinal Chemistry Letters*, 28(17), pp. 2797-2806.

Tok, F. et al., 2021. Synthesis of new hydrazone derivatives and evaluation of their monoamine oxidase inhibitory activity. *Bioorganic Chemistry*, 114, pp. 1-11.

Xie, J. et al., 2020. Synthesis and antiviral/fungicidal/insecticidal activities study of novel chiral indole diketopiperazine derivatives containing acylhydrazone moiety. *Journal of Agricultural and Food Chemistry*, 68(20), pp. 5555-5571.

Yeye, E.O. et al., 2023. In silico studies and antimicrobial investigation of synthesised novel *N*-acylhydrazone derivatives of indole. *Scientific African*, 19, pp. 2468-2276.

Yonis, A. and Awad, G.E.A., 2020. Utilization of ultrasonic as an approach of green chemistry for synthesis of hydrazones and bishydrazones as potential antimicrobial agents. *Egyptian Journal of Chemistry*, 63(2), pp. 599-610.

Yuan, W. et al., 2019. Indole-core-based novel antibacterial agent targeting FtsZ. *Infection and Drug Resistance*, 12, pp. 2283-2296

Zhao, Z.X., Cheng, L.P. and Pang, W., 2018. Green synthesis of ethyl oxalate benzylidinyl hydrazides. *Tetrahedron Letters*, 59(21), pp. 2079-2081.